EINDHOVEN UNIVERSITY OF TECHNOLOGY

Actuator and control design for the plasma needle

Citation for published version (APA):
van Aaken, R. J. T., Bogemann, S. R., Hendriks, F., & de Waal, S. A. J. (2006). *Actuator and control design for the plasma needle*. (DCT rapporten; Vol. 2006.089). Technische Universiteit Eindhoven.

Document status and date:
Published: 01/01/2006

Document Version:
Publisher's PDF, also known as Version of Record (includes final page, issue and volume numbers)

Please check the document version of this publication:

• A submitted manuscript is the version of the article upon submission and before peer-review. There can be important differences between the submitted version and the official published version of record. People interested in the research are advised to contact the author for the final version of the publication, or visit the DOI to the publisher's website.
• The final author version and the galley proof are versions of the publication after peer review.
• The final published version features the final layout of the paper including the volume, issue and page numbers.

Link to publication

General rights
Copyright and moral rights for the publications made accessible in the public portal are retained by the authors and/or other copyright owners and it is a condition of accessing publications that users recognise and abide by the legal requirements associated with these rights.

• Users may download and print one copy of any publication from the public portal for the purpose of private study or research.
• You may not further distribute the material or use it for any profit-making activity or commercial gain
• You may freely distribute the URL identifying the publication in the public portal.

If the publication is distributed under the terms of Article 25fa of the Dutch Copyright Act, indicated by the "Taverne" license above, please follow below link for the End User Agreement:

www.tue.nl/taverne

Take down policy
If you believe that this document breaches copyright please contact us at:

openaccess@tue.nl

providing details and we will investigate your claim.

Download date: 16. Nov. 2023

Technische Universiteit Eindhoven, department of Mechanical Engineering

Master team project

Actuator and control design for the plasma needle

Report number: DCT-2006/89

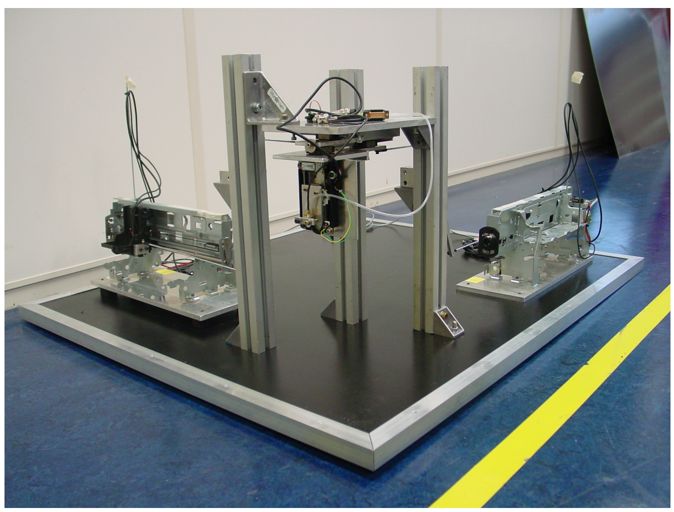

Tutor P.W.J.M Nuij.

Students:
Rien van Aaken 0527535
Sander Bögemann 0534969
Ferdinand Hendriks 0538477
Bas de Waal 0527562

DCT-nr. 2006.089
Date 10-07-2006

Introduction

From different researches ([1], [2]), it has become clear that treatment of skin and teeth is possible with plasma. More specific it does concern burns of the skin and germs that cause plaque. The active parts of the plasma such as electrons, ions, active radicals and excited molecules are responsible for the effect of the treatment. The parts very locally induce apoptosis (suicide) or necroses (instant death) of a cell. Herewith, treatment of tissue without scars is possible. Furthermore, the contact less treatment makes it painless.

To make treatment of patients possible, an actuator has to be designed. This actuator makes it possible to move the plasma needle in x,y,z-direction. During the treatment it is necessary, that the plasma needle is located at a specific distance from the tissue. Only a small deviation of this distance is allowed. The assignment for this Master Team Project can be subdivided in three parts. The first sub-assignment is a redesign of the plasma needle, because the old plasma needle is too large and too heavy. The second point is the application of the plasma needle as a height sensor. To get the distance from the tissue, a height sensor is needed, which can measure the height contact less.

To be able to actuate the plasma needle in x, y and z-direction, an actuator has to be designed and controlled. The exact requirements for the sub-assignments are given in the chapters 2 and 3.

First a small introduction is given with regard to the matching network. In the second section an overview is given of the developments on the new design of the plasma needle. The next chapter gives an explanation of the designed construction, whose controller will be discussed in section 4.

1.Matching Network

To discharge the helium at the tip of the wire in the plasma needle a high frequency electrical field is used. To maximize the energy of the electrical field at the needle tip, a matchbox is needed. To explain why such a device is needed, first some basic concepts of high frequent AC signals are explained. After this there will be dealt with the practical implementation.

1.1 Phasors

A phasor is a complex number which represents the complex amplitude (magnitude and phase) of a sinusoidal function in time. For example take a sinusoidal function y (1.1).

$$y = A \cdot \cos(\omega t + \phi) \tag{1.1}$$

Where A is the amplitude of this sinusoid, and ϕ the phase shift. The angular velocity (rad/s) is represented by ω. This sinusoidal function can be represented as a complex number (1.2).

$$\begin{aligned} y &= \Re(Ae^{j(\omega t+\phi)}) \\ y &= \Re(Ae^{j\omega t}e^{j\phi}) \\ y &= \Re(AYe^{j\omega t}) \end{aligned} \tag{1.2}$$

Where $\Re$ represents the real part of a complex number. And Y represents the phase angle of y (1.3)

$$Y = e^{j\phi} \tag{1.3}$$

1.2 Impedance

The impedance of a system is defined as the total opposition that the system presents to an AC signal. The impedance can be written as a phasor: $Z = R + jX$. The real part R of this phasor is called the resistance and the imaginary part X is called the reactance.

The impedance of three important components of an electronic circuit are given:

- *Resistor* A resistor does not change the phase of a signal and therefore has no imaginary part. The impedance of a resistor can therefore be written as: $Z_R = R$
- *Capacitor* A capacitor creates a 90 degrees phase delay in a signal and therefore it is impedance is $Z_C = 0 + jX_C$, where $X_C = -1/\omega C$.
- *Inductor* An inductor creates 90 degrees phase lead, therefore its impedance is $Z_L = 0 + jX_L$, where $X_L = \omega L$

The impedance of a capacitor and an inductor depends on the angular frequency of a signal.

When all the components of a system are arranged in series, the individual impedances can be added to find te total impedance (2.4).

$$Z_{Tot} = \sum Z_i \tag{1.4}$$

When components of a system are connected in parallel, the total impedance for this system can be found by using the admittance.

$$Y = 1/Z \tag{1.5}$$

The individual admittances can be summed to find the total admittance. The total impedance can then be found by inversing the admittance.

1.3 Transmission line

To transport the AC signal from the RF power supply to the plasma needle a transmission line is needed. A transmission line can be represented by a number of inductors (ΔL) in series and parallel capacitors between the conductors (ΔC) (figure 1.1).

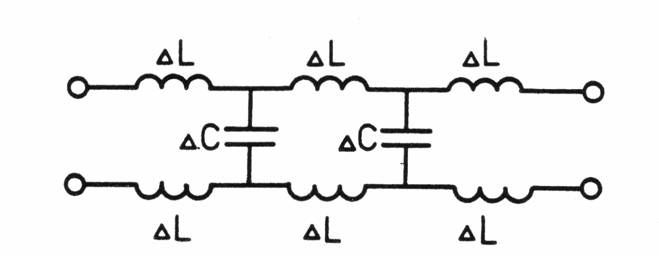

Figure 1.1 Schematic representation of a transmission line

The characteristic impedance of a transmission line is $Z_0 = \sqrt{L/C}$ [3] in this formula there is no angular velocity ω present, the impedance is independent of the frequency.

In the setup a coaxial cable with a length of 50 cm. and a characteristic impedance of 75 Ω is used.

1.4 Reflection coefficient

If an AC signal is lead through a transmission line with a load connected at its end equal to its impedance (figure 1.2), the voltage and therefore the current will be the same all over the line. This is called a traveling wave.

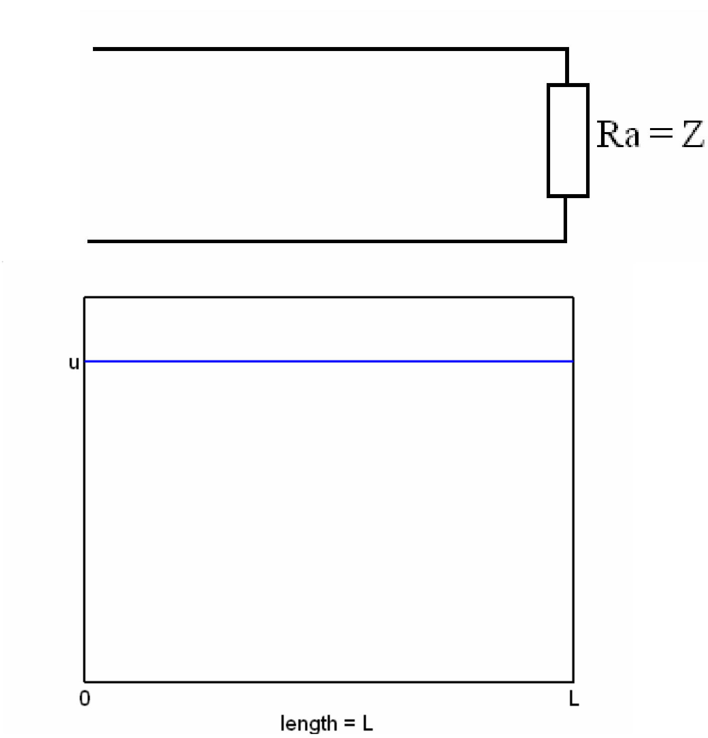

Figure 1.2 Transmission line with right load connected

If an AC signal is lead through a transmission line which has no load connected to it (figure 1.3). The wave traveling through the line will find no user at the end and will travel back through the line. This will result in a standing wave in the transmission line with a maximum voltage at the end of the line. Depending on the length of the line, all possible voltages can be found at the beginning of the line. This variable current and voltage wave is called a standing wave. There is always a standing wave present in a transmission line when not all the power is used at the end of the line and therefore a reflected wave is present.

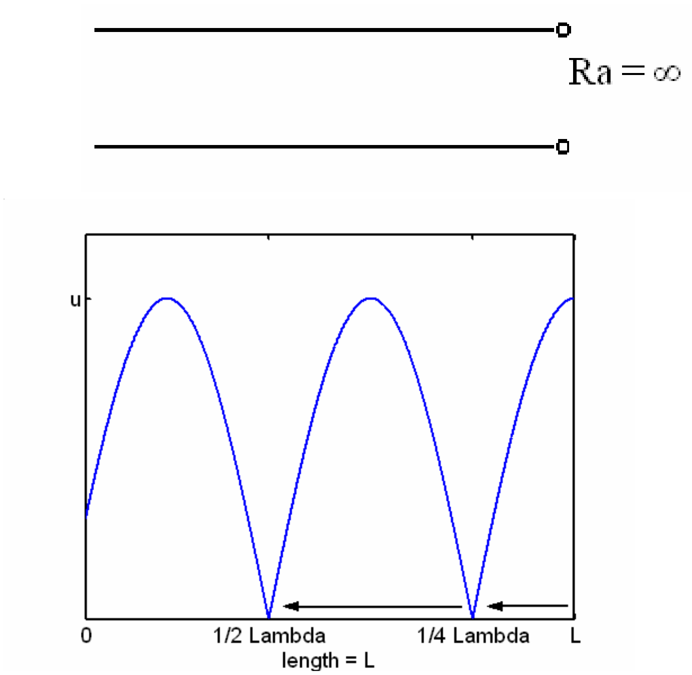

Figure 1.3 transmission line with no load connected

There will be situations in between those above mentioned above. The place in between is located using the standing wave ratio. This is the ratio between the highest and lowest voltages found on a transmission line, also known as the reflection coefficient.

$$\Gamma(x) = \frac{V\max}{V\min}$$

When the impedance of the load and the line are equal, the reflection coefficient is zero.

The power in a system is proportional to the square of the voltage. Therefore the absolute value of the reflection coefficient squared is equal to the reflected power divided by the forward power. [4]

$$|\Gamma(x)|^2 = \frac{P_{refl}(x)}{P_{forw}(x)}$$

1.5 Practical implementation

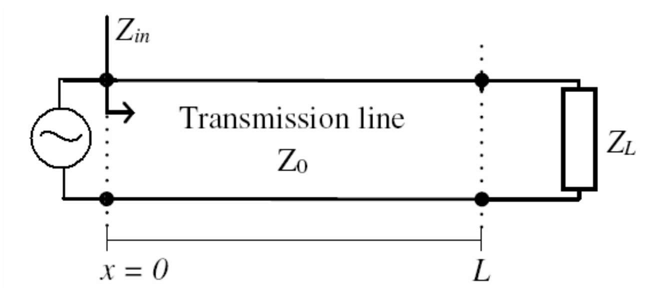

Figure 1.4 A load connected to a power supply with a transmission line

A source will transfer its maximum power if the impedance of the load is equal to the internal impedance of the power supply and that of the transmission line. $Z_{in} = Z_0 = Z_L$.The resistance, the RF power supply sees, also known as the input impedance has to be purely ohmic without any reactive parts. Therefore the reactive parts of the impedance of the plasma needle that might be present have to be cancelled (compensated) and the resistance has to be transformed to be equal to that of the source.

The reactance of a capacitor can be cancelled by the reactance of an inductor. This is called resonance since the phase lead and lag of the two elements will be equal and the signal resonates between the two elements. Since both reactances are frequency dependent this cancellation will only take place at a specific frequency.

The frequency of the RF power supply is 13.56 Mhz, a worldwide standard for various applications that use RF signals. Since the system works at a specific frequency the reactance of the system can be tuned such that resonance takes place.

The impedance of the RF power supply is 75 Ohm in our case. This is equal to the impedance of the transmission line. The plasma needle also has reactive parts in its impedance [4] which will need to be cancelled, therefore a matchbox is needed.

The matchbox consists of two tunable elements (see figure 1.5). Since capacitors are more reliable in tuning, an inductor is placed in series with a tunable capacitor. In this way, the reactance of the inductor can be tuned.

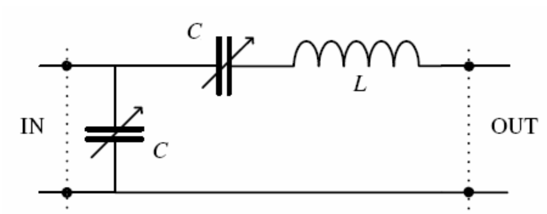

Figure 1.5 Scheme of the variable matchbox

The reflection coefficient can be used to determine if the system is well tuned. With an AR PM2002 power meter, powerheads model PH2000 and powercoupler with serial number 303217 the forward and reflected power can be measured. This measurement can be used to calculate the reflection coefficient. When the matchbox is well tuned, the voltage is at its maximum at the plasma needle tip and therefore plasma production will be the most efficient.

2. Development of the plasma needle

2.1 History

It was asked to design a new smaller needle to make it possible to use in e.g. the mouth. In paragraph 2.1, first the old needle briefly will be discussed. After that the working principle of the needle will be explained in paragraph 2.2. In paragraph 2.3, the design of the final needle is discussed. In paragraph 2.4 the testing of the old- and new needle is discussed. Thereafter, a comparison is made of the old- and new needle in paragraph 2.5 and a conclusion is drawn. In paragraph 2.6 recommendations on further development steps are given.

Old plasma needle

The plasma needle (see figure 2.1) as has been used by [4] and [5], consists of a tungsten wire. This is subjected to a high frequent voltage and shielded by a tube made of glass. This tube is contained in stainless steel, which is grounded by a coax cable. The helium enters the stainless steel cover through a flexible tube and flows around the glass tube and the uncovered tungsten tip. Due to the very sharp tip of the wire and the high voltage on it, the strength of the electrical field is locally very high. Therefore plasma is generated at the tip. Furthermore, the ratio of air and helium can be adapted by sliding the Perspex tube in the stainless steel cover.

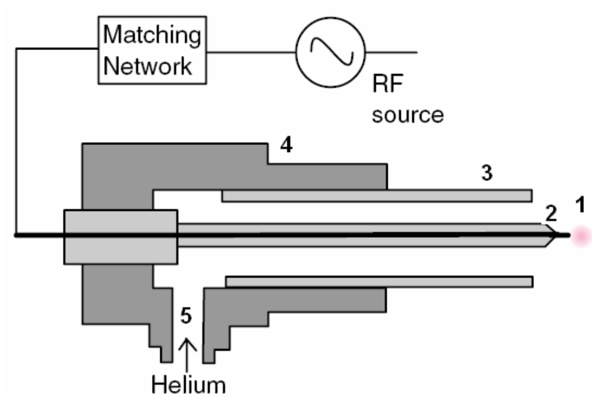

Figure 2.1: old plasma needle

Table 2.1: part description

Part no.	Description
1	Tip of tungsten wire
2	Glass tube
3	Plastic tube
4	Stainless steel cover
5	Helium connection

2.2 Working principle

Plasma will be generated when the helium is subjected to an electrical field with a high fieldline density [3]. For this specific gas, the strength of the electrical field should be at least 2.1e5 V/m. The type of field used at the plasma needle is a so called

"radio frequent, capacitively coupled discharge". Radio frequent concerns the frequency at which the voltage switches (in this case 13.56 MHz). The capacitively coupled discharge is the way the electrical field is generated. In general, by applying a direct current (DC) over two plates, a voltage difference is created. In this case, a pure voltage is put on the wire by an alternating current (AC) source of 10 W. The voltage switches between + 450 V and – 450 V. The surroundings, which can be the air or skin, serve as ground.

Project on the new plasma needle
For demonstration purposes, a prototype was made. It had to deal with some criteria:

1) Reduction of the helium flow (in this way the consumption of helium is reduced, this is important because the price of the gas is quite high)
2) Axial construction (in this way no electrical- or magnetical source is created, it is shielded by the coax cable to reduce RF radiation)
3) Reduction of the weight of the needle (in this way the actuator needs less force to move the needle and can therefore be constructed lighter)
4) Reduction of the size (by reducing the size, the needle can be used in the mouth)
5) Modular construction (in this way the plasma needle can be put on a pencil. The cable and flexible tube should therefore "leave" the needle in an axial manner
6) The needle should be compatible with the existing source and matchbox concerning impedance.

Throughout the weeks, different ideas have been worked out. The most important development steps and the final design are discussed.

2.3 Design of the final new needle

Introduction
After different designs, the needle was taken to the GTD (Gemeenschappelijke Technische Dienst) to be produced. Some small adjustments have been carried out, to overcome shortcomings. They popped up during testing of the needle, as will be discussed in paragraph 2.4.

Basic design considerations
On the basis of the criteria as described above, the needle has been designed (see figure 2.2)

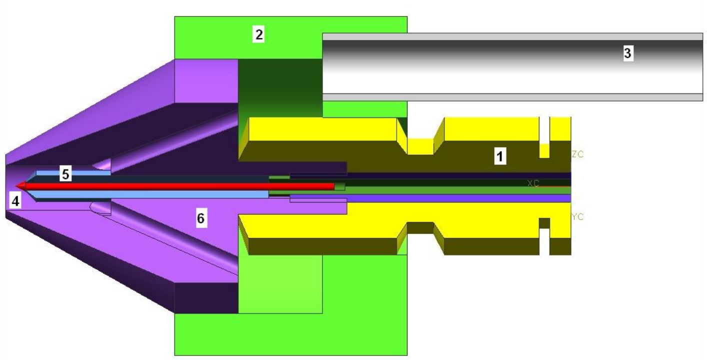

Figure 2.2: design of the final new needle

Table 2.2: description of the final new needle

Part no.	Description
1	SMC-connector (Yellow)
2	Stainless steel cover (Green)
3	Tube for helium (Grey)
4	Tungsten wire (Red)
5	Glass cover (Blue)
6	Teflon cap (Purple)

The starting point for the miniaturisation was the connector. The size of this connector is the limiting factor for the dimensioning. A connector commonly used and in stock by the GTD is a SMC-connector. In the earlier designs, a small male BNC-connector was used, but an extra copper coupling piece was needed to couple the connector to the wire. With the SMC-connector, it is possible to put the tungsten wire directly into the connector. The wire has 2 % Thorium in it, which makes radio-active. This material has been chosen because it can resist the high temperatures of the plasma well and it was present at the GTD. The connector has a coax cable on it, with a length of 50 cm and an impedance of 75 Ohm.
The next step in the design is the dimensioning of the stainless steel cover. It has been chosen to have a large enough diameter to place the connector and the helium tube next to each other. Hereby, the coax cable and the flexible tube for the helium may not interfere. The flexible tube for the helium is a silicon tube with a length of 1 m and an inner- and outer diameter of 2 and 3 mm respectively. Because of the length of the cable, the helium canister does not have to stay next to the needle.
At the front of the needle, a Teflon cap has been placed with a central blind hole of 3 mm in which the wire comes through. To let the helium flow out of this hole, 4 holes with a diameter of 1 mm have been placed axial at an angle of 90 degrees. The angle of those holes with the rotation axis is 30 degrees. In this way, an almost axial flow is created. The connector and the Teflon cap are placed in a stainless steel cover. In between the back of this cover and the cap, there is a helium chamber. In this chamber, the helium has the possibility to scatter in the tangential direction. After that, it can flow equally through the 4 holes. The 4 holes are not in line with the helium tube, but respectively displaced at angles of 45, 135, 225 and 315 degrees as can be seen in figure 3.3. In this way, the helium flow is even more equal.

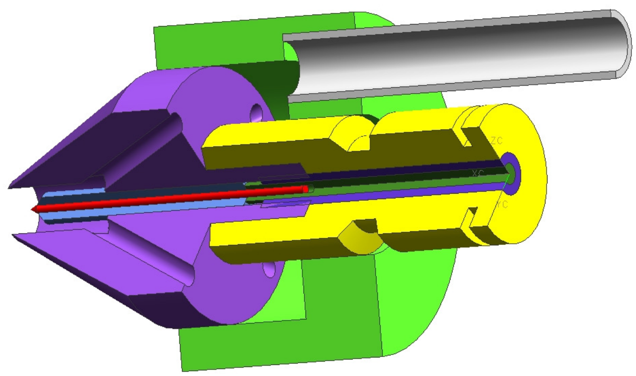

Figure 2.3: placement of the holes in the cap relative to the helium tube

The stainless steel cover has a thickness of 2 mm, using thread the needle can be coupled to a “tail” tube made out of plastic. This thread however is not yet present, because this was not the scope of this project. Teflon and stainless steel were chosen to work with because of the high temperatures they can withstand. In this way they can also withstand the temperature of the sterilization process (at about 150° C) [5]. In appendix G, calculations on the helium flow velocity and pressure drop can be found.

2.4 Testing

The goal of this testing is to examine whether the needle can be used as a sensor to measure the distance of the tip to the skin. Therefore the quotient of the reflected- and forward power $\left(\frac{P_{reflected}}{P_{forward}}\right)*1000$ (from now on called "the quotient") should indicate only one distance.

The testing has been done using a platform (figure 2.4). It consists of a vice made by Newport, onto which the needle is bolted. It has a range of 0-5 mm and an accuracy of 0.05 mm. A metal plate with tape on it represents the electrical resistance of skin. For this, also a little sheet of glass has been used. The needle has been fixed in such a way that the tip of the needle just touches the plate at a range of 0 mm.

Table 2.3: description of testing platform

Part no.	Description
1	Plasma needle
2	Plate (representing skin)
3	Fixed ground
4	Vice

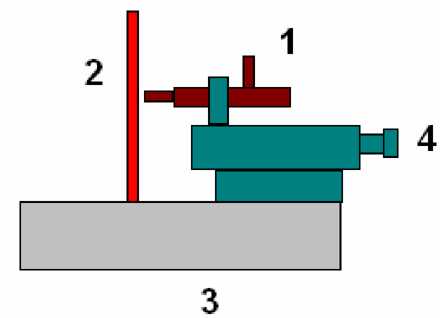

Figure 2.4: testing platform

Testing the old needle

It was observed that the forward power $(P_{forward})$ at the needle had to be at least 2 W to sustain the plasma. Further measurements learnt that a power of at least 4 W had to be used, otherwise the measurement data fluctuated. This probably indicates unstable plasma. The forward power may not exceed 5 W however, because this induces a destruction of cells. The power consumed by the cells in that case exceeds 300 mW. In figure 2.5, a typical quotient of the old needle can be seen.

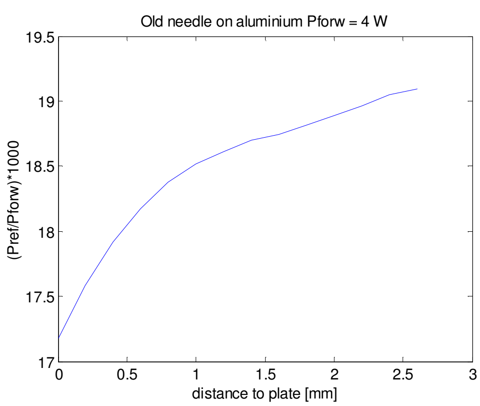

Testing conditions	
Distance [mm]	Varying
P_{forw} **[W]**	4
P_{ref} [mW]	About 72
Helium flow [L/min]	0.6
Type of matchbox	small
Skin representation	Aluminium+tape

Figure 2.5: quotient of old needle, P_{forw} = 4 W, aluminium plate

Because of the distinguishable quotient at each distance and an inclination angle of the quotient unequal to 0 at 2 mm, this needle can be used as a sensor.

Testing the new needle with Teflon cover

The first needle had a Teflon cover of the wire. Only 1 mm of the tip of the wire is uncovered. This needle needed a forward power of at least 6 W to make a more or less stable plasma. Because of the lower helium flow and the smaller design when compared to the old needle this was not expected. Figure 2.6 represents a typical quotient of this needle at a forward power of 8 W.

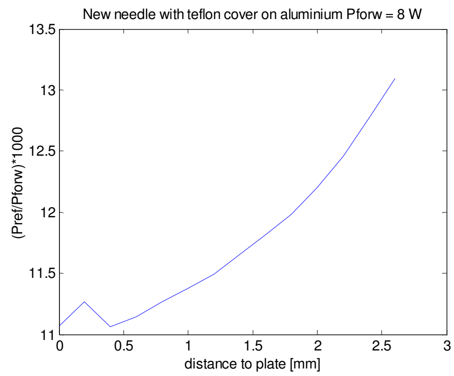

Testing conditions

Distance [mm]	Varying
P_{forw} **[W]**	8
P_{ref} [mW]	About 88
Helium flow [L/min]	0.6
Type of matchbox	small
Skin representation	Aluminium+tape

Figure 2.6: quotient of new needle, Teflon cover, P_{forw} *= 8 W, aluminium plate*

From figure 2.6 it can be seen that the needle can be used as a sensor when the skin is represented by an aluminium plate with tape on it. To validate whether the needle would also work on other representations of skin, a sheet of glass has been used. In figure 2.7 a typical representation of the quotient of the needle on glass can be seen.

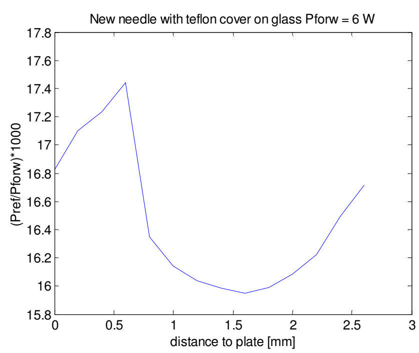

Testing conditions

Distance [mm]	Varying
P_{forw} **[W]**	6
P_{ref} [mW]	About 101
Helium flow [L/min]	0.6
Type of matchbox	small
Skin representation	glass

Figure 2.7: quotient of new needle, Teflon cover, P_{forw} *= 6 W, glass plate*

It is very obvious that this behaviour of the needle cannot be used as a sensor. Selecting one value of the quotient can mean that the needle is at two distances from the skin. To solve this, one could look at the derivative of the quotient but this is too difficult. Furthermore, the sign of the quotient alters sharply at a distance of about 0.6 mm. This probably has to do with the presence of plasma at the wire before the tip. Not only does the skin function as ground, also the helium surrounding the wire does. In that case, the sensitivity of the sensor decreases. This is because the impedance change of the plasma due to a change in distance is relatively smaller when plasma is already present around the wire and not only at the tip. Because the theory about the existence of the electrical field was not clear at that time, it was decided that a glass tube with an (in advance unknown wall thickness) had to be placed around the wire. The wall thickness of this tube is chosen to be 0.5 mm and the wire is about 5 mm long.

Testing the new needle with small glass cover

The front part of the wire is now covered by glass. Still the wire in the connector is uncovered.
From these tests it became obvious that with the same settings for the forward- and reflected power, different quotients could appear. This can be seen in figure 2.8. Not only the behaviour is very different with the same initial conditions, there also seems to be some kind of time effect. This could be caused

by warming up effects of the electronics (especially the matchbox) or pollution of the surface of the needle. The longer one is measuring, the more the line of the quotient is drifting in an upward direction.

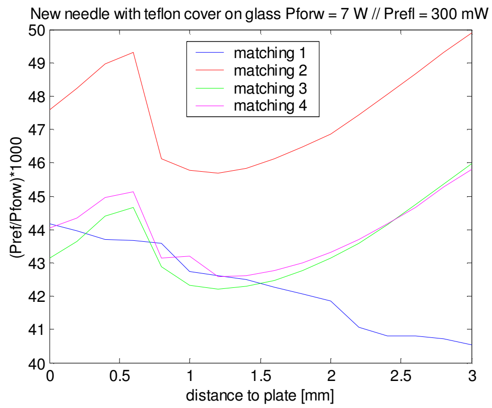

Testing conditions

Distance [mm]	Varying
P_{forw} **[W]**	7
P_{ref} [mW]	About 300
Helium flow [L/min]	0.6
Type of matchbox	small
Skin representation	glass

Figure 2.8: quotient with glass cover, $P_{forw} = 7$ *W,* $P_{refl} = 300$ *mW, glass plate*

Because of this very strange behaviour the matchbox of Ewout van der Laan has been used to check whether this would make a difference. It has the ability to vary the capacity of the capacitors more than the new matchbox; the matching of the needle with the matchbox would probably cause the changes of signs in the quotient and maybe the heating up.

Testing the new needle with filled connector and glass cover

Because this needle heated up especially at the connector, we thought plasma was also generated in the connector. Therefore (as can be seen in the final design), the connector is filled with Teflon and the needle is covered by glass. After that, warming up of the needle itself only occurred at high forwarded powers and mismatching. With the operational powers applied later, this did not occur. With this configuration, tests have been done with the matchbox of Ewout van der Laan. From these tests, it became clear that also with this matchbox a time effect was present. The quotient drifts when measurements are done with the same settings with a time in between the measurements of about 30 minutes. After 5 hours op warming up, new tests have been done. They show results as can be seen in figure 2.9.

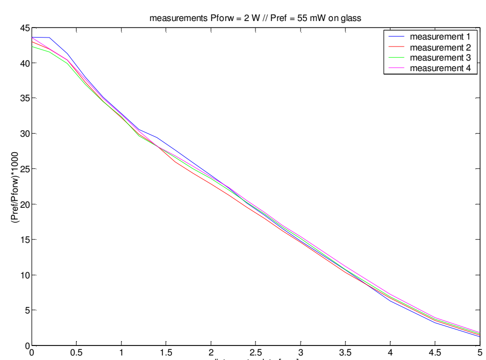

Testing conditions

Distance [mm]	Varying
P_{forw} **[W]**	2
P_{ref} [mW]	About 55
Helium flow [L/min]	0.6
Type of matchbox	large
Skin representation	glass

Figure 2.9: quotient with glass cover, $P_{forw} = 2$ *W,* $P_{refl} = 55$ *mW, glass plate*

From these measurements, one can see that there is no temperature - or time dependency anymore. Still, fluctuations occur in the forward- and reflected power even at one distance in one measurement, probably caused by unstable plasma. Further research has to be done on this subject.

To cope in a control point of view with these fluctuating values, a low-pass filter has to be implemented or averaging has to be done. The quotient at the working distance of 2 mm is also of importance, the question is whether the needle can be used as a sensor. This can be seen in figure 2.10:

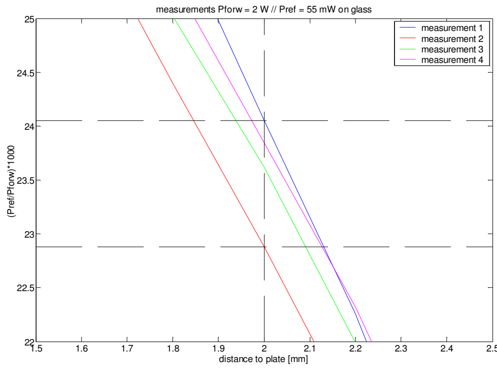

Testing conditions

Distance [mm]	Varying
P_{forw} **[W]**	2
P_{ref} [mW]	About 55
Helium flow [L/min]	0.6
Type of matchbox	large
Skin representation	glass

Figure 2.10: quotient with glass cover, Pforw = 2 W, Prefl = 55 mW, glass plate

From this figure it can be seen that after 5 hours of heating up, the quotients have almost the same inclination angle. To conclude whether the needle can be used as a sensor, the highest (24.05) and lowest values (22.88) for the quotient at 2 mm are taken. Those values are represented with the horizontally dotted black lines. After that, an “average quotient” has been taken and the crossings with both dotted lines are looked for. It turns out that the crossings occur at distances of respectively 2.09 mm and 1.939 mm. This is well in the range of the 10 % margin (0.2 mm from the working point of 2 mm) as stated in the requirements.
Because the sensor acts relatively, the only extra disturbances from the forward - and reflected power may come from data-acquisition or delay. Also the electrical resistance of the skin may affect the characteristic of the needle. When that occurs, a new quotient has to be measured specifically for that application. Furthermore, plasma still occurs around the wire. This means that the wall thickness of the glass tube is not large enough to reduce the electrical field sufficiently. The calculation of the electrical field is dealt with in Appendix F. The generation of plasma around the wire probably reduces the sensitivity of the sensor.

2.5 Designing

Design of the needle with Teflon cover
Because plasma can occur around the wire, this has to be prevented. This can be done by using a cover. First it is chosen to use Teflon for that. Teflon has a lower breakthrough voltage of 20 kV/mm [6]. Because the highest voltage used at the wire is only 450 V and the Teflon cover had a thickness of about 0.1 mm it should be sufficient. This however was a misconception because it only holds for direct current. The alternating current will travel through the cover and does not feel its resistance. Therefore plasma still occurred around the wire. Because plasma only occurs when an electrical field is applied and glass is more effective to lower this field glass is used.

Design of the needle with small glass cover
By applying a tube of glass of about 5 mm and a wall thickness of 0.5 mm, the electrical field should reduce. With these dimensions the tube it would still fit in the old design without that large change. This new configuration is tested also.

Design of the needle with Teflon filled connector and glass cover
Because the needle heated up, it was expected plasma also occurred in the connector. Therefore, the connector is filled with Teflon. The total length of the wire is covered by glass. The glass cover also has a wall thickness of 0.5 mm. At that time, the calculations on the electrical field were not present yet. Later on, calculations on the thickness of the cover are done, which can be seen in appendix F. The design of the needle is discussed in paragraph 2.3.

2.5 Comparison of the old and final new needle

The final design can be compared with the old design as can be seen in table 2.4:

Table 2.4: comparison of old and new needle

Criteria	**Old design**	**Final new design**
Weight [grams]	117	27
Forw. working power [W]	4	2
Refl. Working power [mW]	50 mW	55 mW (1 mW possible)
Helium flow [L/min]	2	0.6
Size l*w*h [mm]	93*18*45	33*16*16
Axial configuration	Yes (BNC connector)	Yes (SMC connector)
Modular configuration	No	Yes (i.c.w. a tube)
Compatible with electronics	Yes (“new” matchbox)	Yes (“old” matchbox)
Useful as a distance sensor	Yes	Yes (with 0.1 mm accuracy)
Production costs per needle [€]	Unknown	About 1100

In figure 2.11, the new and old design can be seen:

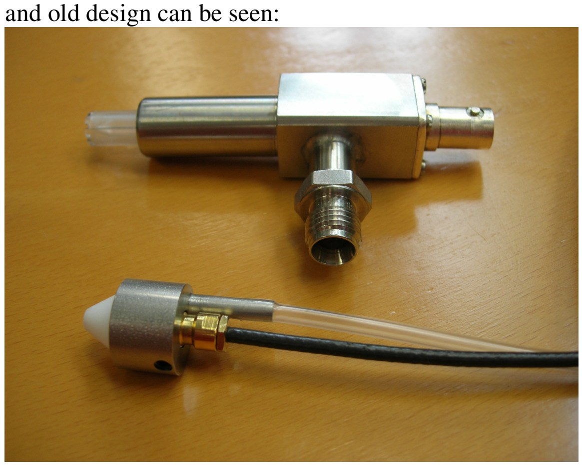

Figure 2.11: old and final new design

To get an idea of the size of the needles, pictures with a “vingerhoedje” on it have been taken. They can be seen in figure 2.12:

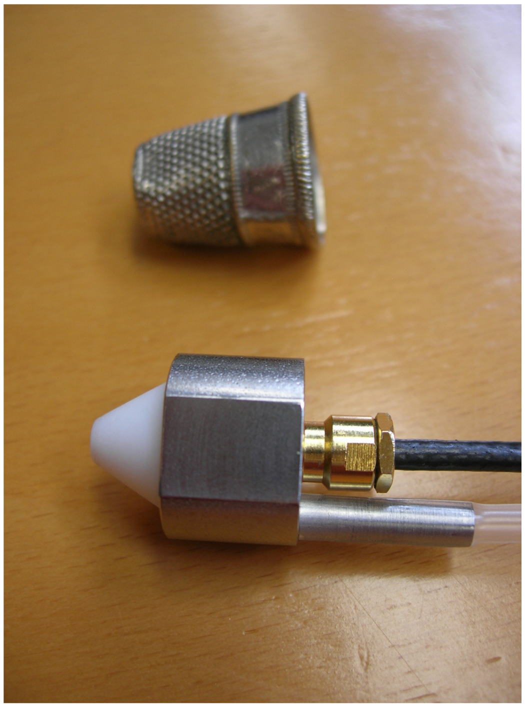

Figure 2.12: new final design

Conclusion

The new design outperforms the old design at weight with about a factor 4 and considering the forward working power with a factor 2. The helium flow has been reduced by about a factor 3. The possible reduction in reflected power is very large, about a factor 50. It was expected that the forward power had a linear relationship with the helium flow, but this was not the case.

The final new needle is able to work as a sensor. It has an accuracy of 0.1 mm which is 2 times better than required. The sensitivity of the sensor is probably reduced by plasma generation inside the plasma needle.

Research on the radial electrical field has therefore to be done. In appendix F, a lower bound has been given for the wall thickness of the dielectric. With the matchbox used by Ewout van der Laan, the reflected power of the new needle can be reduced to very low values. With the large matchbox it was not possible to fine-tune those values because of the lack of accuracy. Furthermore, the adjustment possibilities are also limited. The values for the forward- and reflected power however vary at the same distance, which is probably caused by unstable plasma generation. Therefore, the reflected power has been put from 1 to 55 mW at a distance of 0.0 mm. This did not stop the fluctuation of the powers. Further research has to be done to cope with this. The heating up of the electronics causes a shift of the quotient which affects the accuracy of the sensor. A heating up time of at least 5 hours is required. Working with less power and smaller electric components may reduce this effect.

3. Design of the x, y and z-actuator

Under static and dynamic conditions, the plasma needle has been tested on tissue [4]. To make it possible to move the plasma needle above tissue or skin, an actuator has to be made, which can move the needle in x, y and z-direction. Because we assume only small height differences of the tissue of about 1 mm, we will design a x y z-actuator and not a radial actuator.
By using the plasma needle as a height sensor, the distance from the tip of the needle to the tissue is measured. The plasma takes the shortest way from the tip of the needle to the tissue, assuming an almost flat surface, the shortest distance is the vertical distance.
To treat the tissue or skin, it is necessary to scan the tissue, so every point is treated. This is the movement in x and y-direction. In z-direction, the distance between the tip of the plasma-needle and the surface has to be a specified distance.

3.1 Specifications

The specifications for the actuator are:

- Stroke in x-direction:	40 mm
- Stroke in y-direction:	40 mm
- Stroke in z-direction:	5 mm
- Accuracy in z-direction:	0.2 mm
- Accuracy in x- and y-direction:*	0.5 mm
- Distance above the tissue:	2 mm
- Treatment time tissue:	60 seconds, with a power of 0.2 W
- Scan velocity:**	8 mm / minute
- Prototype must be built within 10 weeks.	
- Low budget, within a budget of 500 Euro.	

* This value is not very sharp, as long every point of the tissue is treated.
** At a distance of 2 mm above the surface, the treated tissue has a circular surface, with a diameter 8 mm. This gives a velocity of 8 mm/ minute en P_{forw}.

To be sure every point of the tissue will be treated for the same time, the strokes have to overlap. The overlap has to be half of the diameter, of the treated surface.
In figure 3.1 an overview is given.

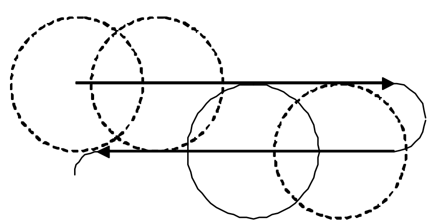

Figure 3.1: overview stroke with overlap

3.2 Design

Degrees of freedom
To fix an object completely, it is necessary to suppress six degrees of freedom, the three translations in x, y and z-direction and the three rotations around these axes. For this actuator, only a movement in three directions is necessary, so the three rotations have to be suppressed. An overview of the coordinate system is given in the next figure.

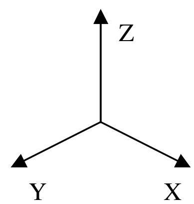

Ideas
The accuracy in x and y-direction do not have to be very large. That is why a simple actuator can be used to actuate the plasma needle.
A possibility to actuate the needle in x and y-directions, is using industrial spindles in both directions. In this way a very exact motion can be made, a disadvantage of these spindles is the very high costs. Therefore it is decided not to use those

Another actuator for this application is an actuator of a printer, because of the accuracy and linear motion. During a previous project the accuracy of a printer, during constant velocity was about 0.1 mm. Some other advantages of using a printer drive are: low costs of secondhand printers, experience with controlling a printer and the presence of a linear encoder. In this way it is possible to measure the position of the head and create a feedback loop. The printers we use for this actuator are manufactured by HP DeskJet. An overview of the print head is given in figure 3.2

In z-direction has a 2 mm distance to the tissue has to be maintained with an accuracy of 0.1 mm. Because of the high accuracy and small forces an actuator of a CD-Rom drive is used. In normal life this actuator positioned the read-head of the CD-Rom drive in radial direction. To actuate the plasma-needle in z-direction the readhead will be replaced by the plasma needle.

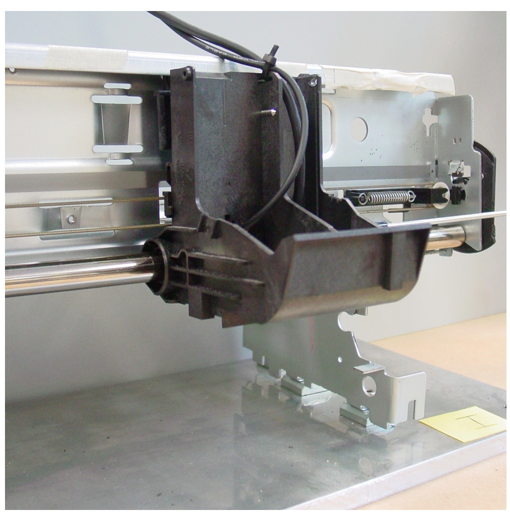

Figure 3.2: write head printer 1, (type HP DeskJet)

Stacking

Using a printer head, it is possible to actuate the plasma needle in x or y-direction. To get a motion in x and y-direction, two printers have to be used. The easiest way is stacking up the two printers. This implies that the first printer is mounted onto the (fixed) ground and the second printer is fixed onto the write head of the first printer. In this way a large mass has to be moved by the first printer. Another problem is the quality of the slides, because they are not strong en rigid enough to support a complete printer. For that reason a construction has to be designed that uncoupled the x and y-direction. In this way both printers can be fixed on the ground.

Slides

Another point of attention are the slides. The linear slide in the printer is not good enough to use, because of the dimensions. The slide length of about 250 mm is far too much for our specifications. That is why is chosen to use other slides. In industry a lot of slides are available; but at high prices. Nevertheless, good slides are of great importance and so it is decided to buy slides, specifications of the slides can be found in appendix B.

Uncoupled movements

Using a printer drive and separated slides, it will be possible to get a movement in x and y-direction without stacking two printers. In this way a small mass has to be moved and the large influence of the stick-slip effects of the printers can be reduced because a larger velocity is possible by using a lever. In this way it is possible to use the cheap drive of a printer and the quality of the slides

3.3 Construction

The most important part of the construction is the decoupling of the motion in x and y-direction. This part will be explained in detail in this paragraph.

3.3.1 Explanation of construction with plasma needle in upward position

The first slide (a) is placed on a plate (b), see figure 3.3. On this plate, the complete construction in x, y and later also z-direction will be placed. The first slide makes it possible to get a movement in x-direction

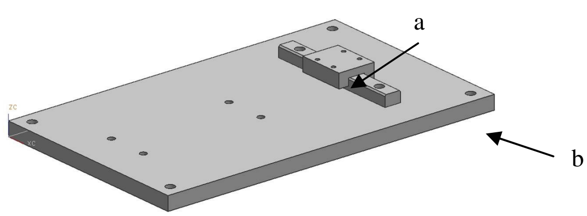

Figure 3.3: plate with first slide

In figure 3.4 the second slide (c) is placed, with an intermediate body (d) on the top of slide one. The two slides are placed perpendicular to each other. The intermediate body can be actuated directly by connecting the printer head to the slide.

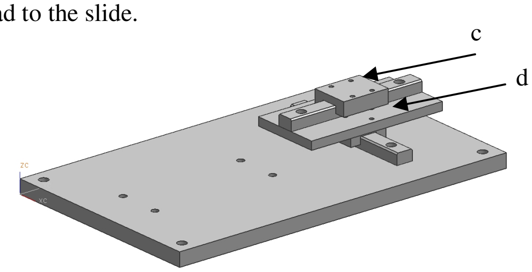

Figure 3.4: second slide is placed perpendicular on the top of slide one

On the second slide, a platform (e) is fixed. On this platform the actuator for the z-direction will be placed. The platform is able to move in x and y-direction, but only the x-direction can be actuated directly by the printer. To make it possible to actuate the platform in y-direction an extra plate (f) is fixed at the left side of the platform. The function of this beam will be discussed later.

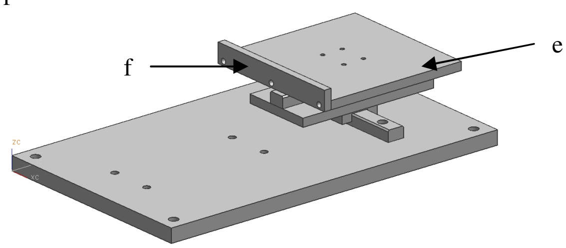

Figure 3.5: platform for placing the z-slide

To make it possible to drive the platform in y-direction an extra slide (g) has to be used. The slide is placed on a block (h), to get the right height, see figure 3.6. On this slide an extra body (i) is fixed, on which a bearing (j) has been placed. This bearing can rotate freely around the z-axis and is placed on the intermediate block. When the slide moves in positive y-direction (see arrow Y in figure 3.7), the bearing is pushing against the platform. At the moment the first slide moves the platform in x-direction (see arrow X), the wheel rolls over the beam. In this way the two x and y-direction are decoupled.

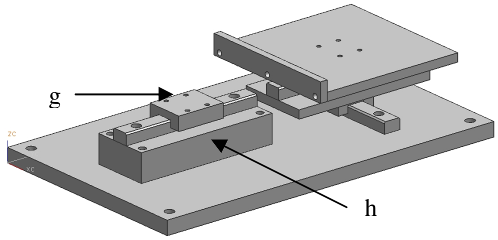

Figure 3.6: construction with third slide

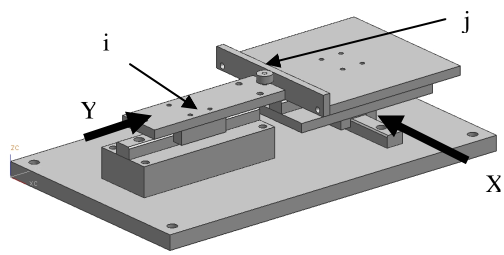

Figure 3.7: intermediate body and bearing added

To make it possible to move the platform in negative y-direction a construction has to be designed, which provides constant contact between the platform and bearing. In this design a lever (k) has been chosen, with at the end a bearing (l) (figure 3.8 and 3.9). The lever is pushed against the other side of the plate by a spring (m) (see figure 3.9)

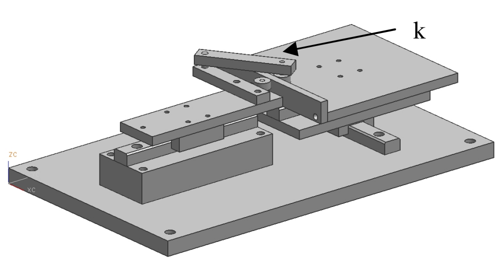

Figure 3.8: construction with beam

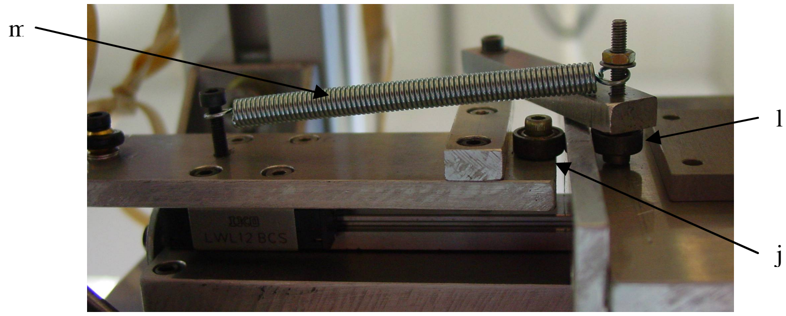

Figure 3.9: construction with spring

The stiffness of the connection in positive y-direction is equal to the stiffness of the bearing just as the stiffness of the axle which connects the bearing and the intermediate body. The bending stiffness of the beam will be neglected.
In negative y-directions the stiffness is equal to the spring stiffness. If a spring is chosen with a very high stiffness between the platform and the third slide the connection can be expected to be rigid

3.3.2 The z-direction

To actuate the needle in z-direction, a third slide has to be placed on the platform, witch can move in x- and y-direction. For the z-slide a CD-Rom actuator will be used. The complete drive will be; the slide electromotor and end switch. The end switch is used to get a zero point for initializing.

To fix the actuator, a supporting profile (n) will be used. On this profile, a thin plate is fixed, to make it possible to mount the CD-Rom actuator

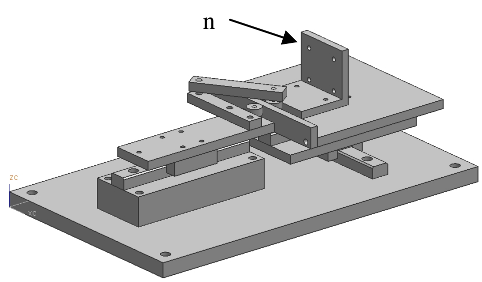

Figure 3.10: construction with supporting profile

In figure 3.11, the complete z-drive is depicted. Here in the motor (o) and the slide (p). The end switch is given by q. The function of the end switch will be given in chapter 3.3.5. The complete construction has been rotated 180 degrees. In this way, the plasma needle sticks out and can scan the surface.

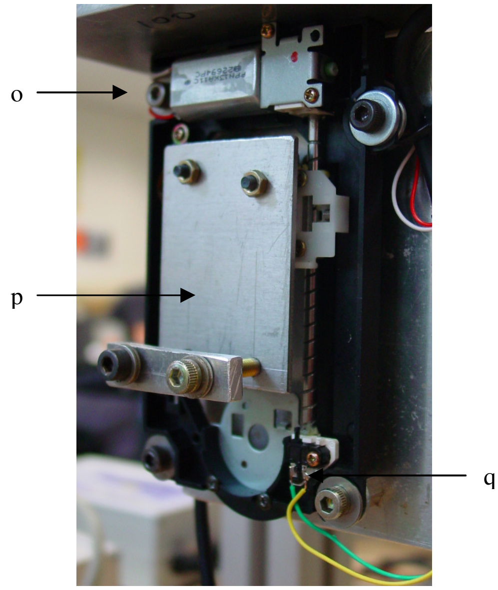

Figure 3.11: z-slide

3.3.3 Fixing the plasma needle

The plasma needle has to be fixed on the z-slide. To make this possible a flat side has been made on the new plasma needle. The flat side prevents the cylinder from rolling during fixing. On the upper side of the cylinder, a strip (r) connected with two bolts pushes on the plasma-needle, see figure 3.12.

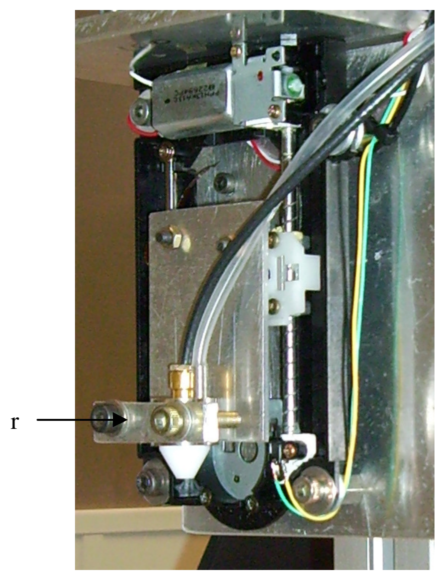

Figure 3.12: Plasma needle fixed on z-slide

3.3.4 The levers

Using printers to drive has a lot of advantages, but also some disadvantages. The biggest disadvantage is the stick-slip effect. Because of the very low velocity the stick slip situation will have to be overcome constantly. To get a bigger velocity of the printer, a lever is used, see figure 3.13. The ration of this lever is 1/3. The lever is placed in a vertical position to make it possible to mount the two printers and the z-stage on a plate.

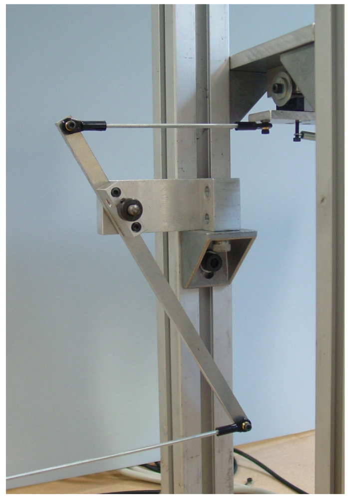

Figure 3.13: lever

3.3.5 The end switches

When power is put on the printer, the slides have to initialize first. To make this possible a switch is placed at the end of the stroke of the printer. At the moment, the slide will be moved slowly in the direction of the switch and hits the switch, the printer knows where the slide is. From this point, the "real" movement can start.

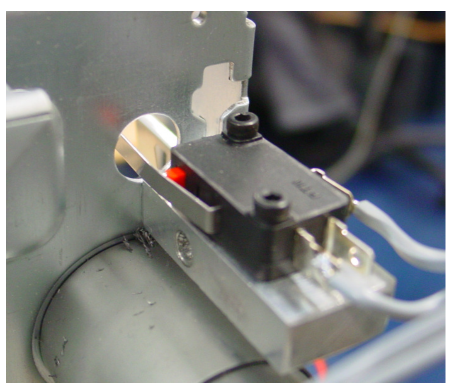

Figure 3.14: end switch

3.3.6 The complete construction

Assembling all different components, gives an x, y, z-actuator for the plasma needle. An overview of the construction is given in Figure 13. The costs of all the components, without the plasma needle are 225 Euro.

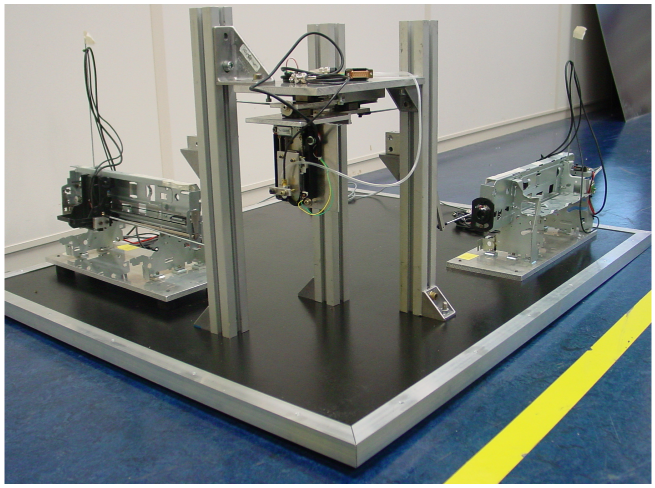

Figure 3.15: overview construction

3.4 Dynamic analysis actuator

To get insight in the dynamic properties of the x,y,z-actuator, a dynamic model has been made. This model is given in appendix D. In this model the masses, stiffnesses and clearances are determined or estimated. In this way the lowest natural frequency can be determined.
Using the parameters in appendix D, calculations are done, related to the lowest natural frequency. For this calculation the equivalent mass and stiffness have to be calculated.

$$\omega = \sqrt{\frac{m_{eq}}{c_c}} \Rightarrow f = \frac{1}{2\pi}\sqrt{\frac{m_{eq}}{c_c}} \qquad (3.1)$$

To calculate the equal mass, al masses have to be counted. Some masses have to be corrected for the ratio of the lever, using formula 3.1.
Also the stiffnesses have to be used to correct the masses. Using formula 3.2, gives the equal mass.

$$m_{eq} = m'_1 + m'_i \left(\frac{\frac{1}{c'_i} + \ldots \frac{1}{c'_n}}{\frac{1}{c_c}} \right)^2 + \ldots + m'_n \left(\frac{\frac{1}{c'_n}}{\frac{1}{c_c}} \right) \qquad (3.2)$$

In formula 2, C_c is equal to the replacement stiffness; this stiffness can be calculated with formula 3.3.

$$\frac{1}{c_c} = \sum_{i=1}^{n} \frac{1}{c'_i} \qquad (3.3)$$

Table 3.1: Results printer 1 and 2

	Printer 1	Printer 2
Equal mass [kg]	0.54	0.57
Replacement stiffness [N/m]	2.41e4	3.17e4
ω_{eigen} [rad/s]	210.7	234.9
f_{eigen} [Hz]	33.5	37.5

4. Controller

An x,y,z-actuator for the plasma needle has been made. Of course this actuator has to be controlled before it can be used. To do so the following equipment has been used.

The actuator as it is described in chapter 3 of this report. An external DC power supply to supply the light valve of the printers with power. Three amplifiers are used to supply the drives of the printers and the cd-rom drive with enough power. To generate the signals for the drives and to measure the signals from the encoders and powerheads, TUeDACS are used. The processing of the data and the measurements have been done with a NEC Versa P520 portable computer with MATLAB 6 and a Linux Knoppix 3.6 operating system.

For the control of the z-direction also the plasma needle, as it has been described in chapter 2 of this report, has been used. To regulate the flow of the helium, that is necessary for the plasma needle to work, a flowcontrol is used. A RF power supply is used to generate the RF signal that is needed to generate plasma. To match the impedance of the power supply with the plasma needle, a matchbox is used. To measure the forward and reflected power to and from the matchbox and the plasma needle, powerheads are used.

4.1 Control in x- y direction

The control loop of the x and y actuator is modeled as shown in figure 4.1. In the figure, r represents the reference, e the error, C(s) the controller, d disturbances, u input of the system, H(s) the system and y represents the output. The identification of the system is done with a so-called Frequency Response Function (FRF) Measurement. The best way to do this is to measure the Sensitivity (S) and the Process Sensitivity (PS). The S is the response from d to u; 1/(1+CH). The PS is the response from d to e; H/(1+CH). By dividing PS by S the system can be found.

The ‘disturbance’ in this measurement is self-made, so it can be measured and a response can be calculated. The disturbance added to the control loop is a white noise. This noise contains all frequencies, so a response of all frequencies can be made. A problem with this method is that a controller is needed because of the closed loop, which is on the edge of stability for a mass-system like this. To avoid instability, a low-bandwidth controller is made (~3Hz).

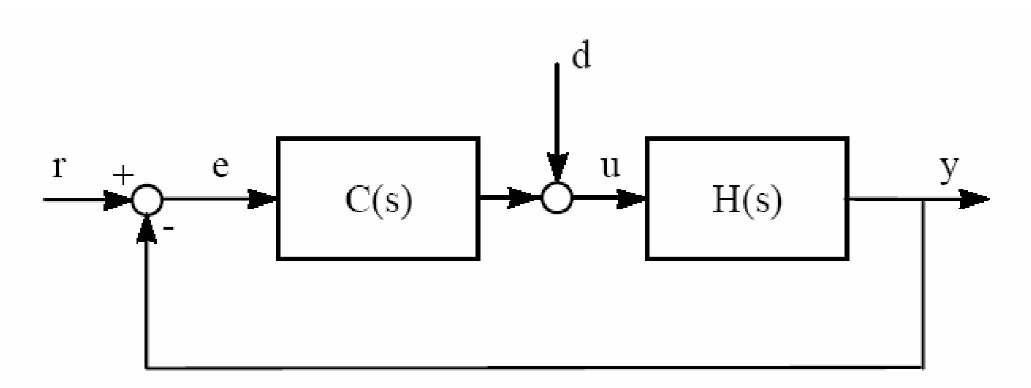

Figure 4.1: overview model control loop

To avoid non-linear effects like stick-slip, the reference is a sine. The results of such measurements for printer 1 are shown in figure 4.2. The typical -2 slope is clearly visible between 10 and 50 Hz. Resonances occur from 30 Hz on upwards. This corresponds with the theoretical eigenfrequencies, as described in chapter 3.4.

Because the actuation in x and y direction is perpendicular, one would expect that they are almost completely decoupled. To check this, more than 1 FRF measurement is done. For each measurement of a stage, the other one is put on another position. If the outcome is the same for all the measurements, the actuation is decoupled. This is also shown in figure 4.3.

Printer 2 differs a bit from printer 1, but shows the same overall characteristics.

The designed controllers are lead-controllers to get some phase margin. The controllers are designed such that the system has a bandwidth of approximately 20 Hz. To check stability, Nyquist plots have been made. For robustness reasons the open-loop transfer function (CH) should be at a distance of at least 0.5 from the point (-1,0) in the Nyquist plot. This can be seen in figure 4.4 and figure 4.5 for printer 1 and printer 2 respectively.

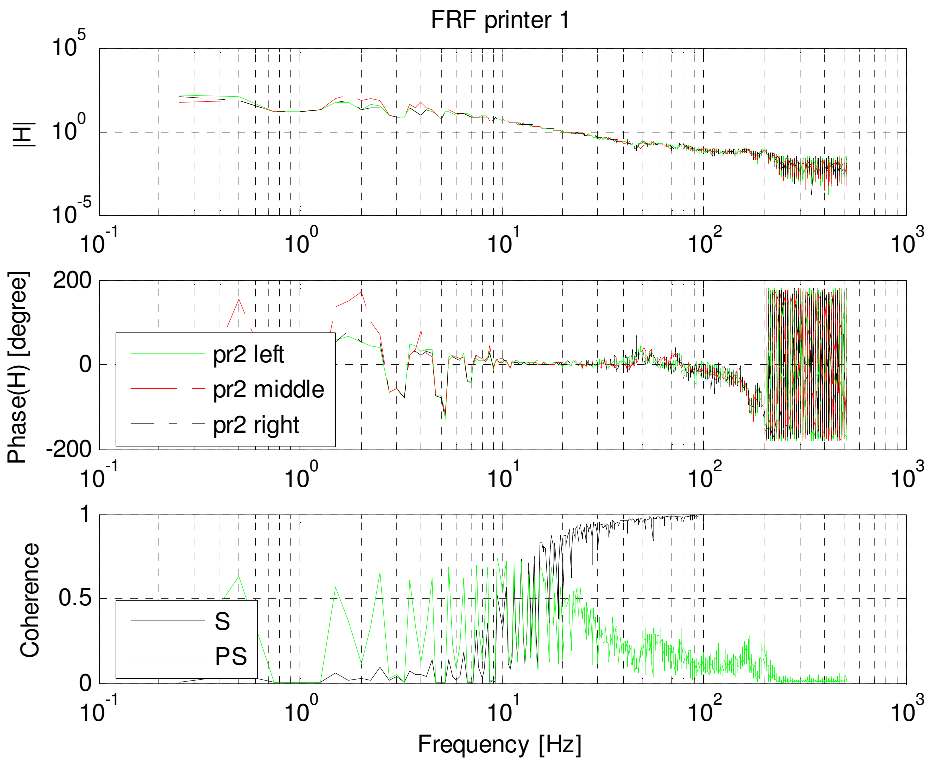

Figure 4.2: FRF printer 1 shows the system is decoupled

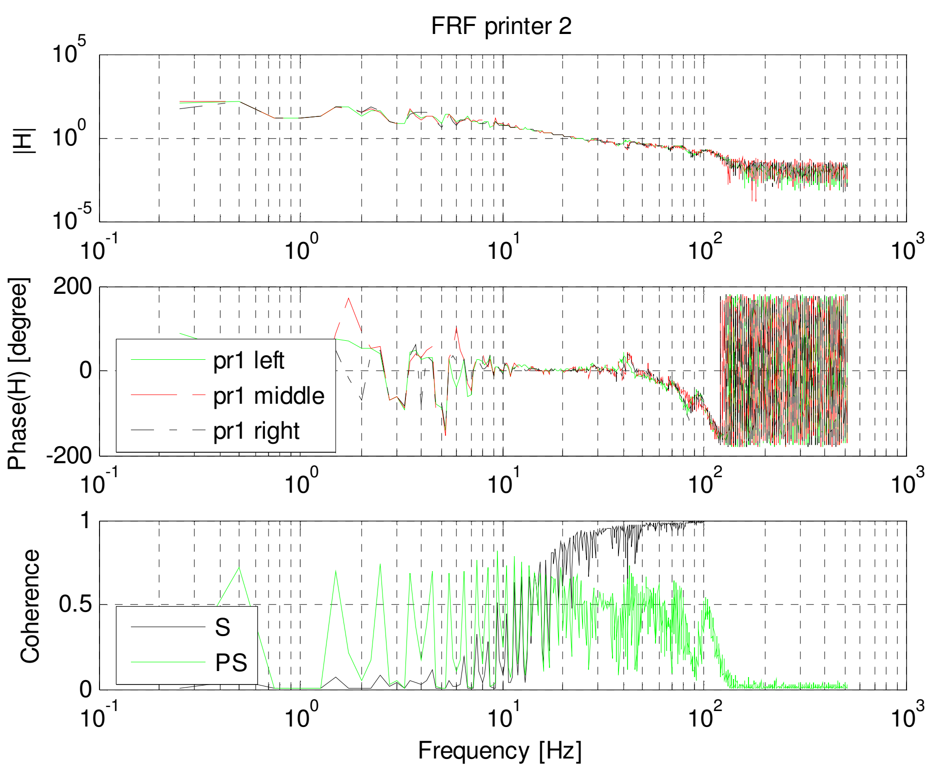

Figure 4.3: FRF printer 2 shows the system is decoupled

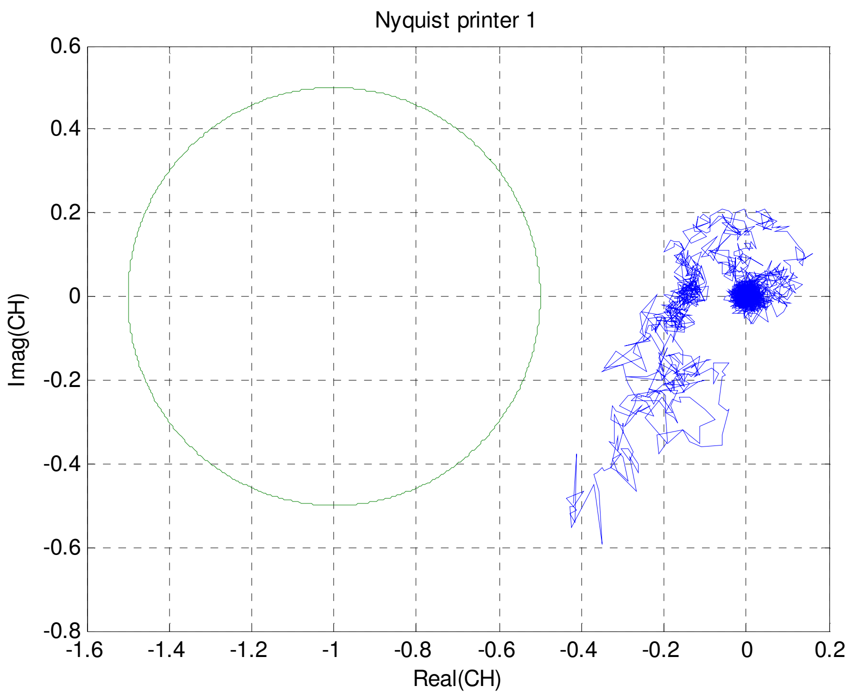

Figure 4.4: nyquist plot printer 1 shows stability

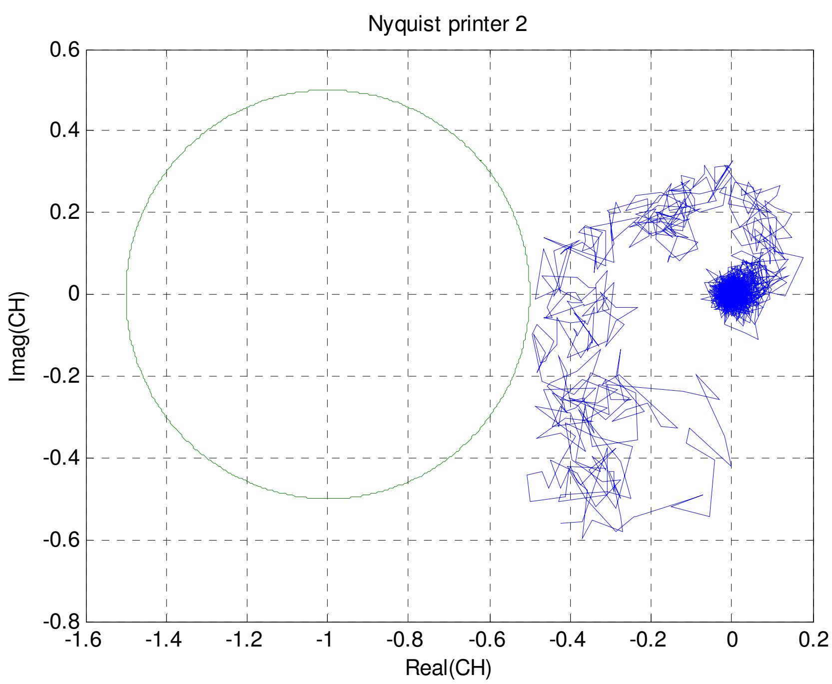

Figure 4.5: nyquist plot printer 2 shows stability

With the designed controller the x- and y slides can be moved well at a reasonable speed for printers, this is very fast for our setup. Moving very slow is problematic because of the stick slip. To reduce the error, a mass-feedforward and a velocity-feedforward are designed. The virtual 'mass' of the system is determined by fitting a line through the FRF, as can be seen in figure 4.6.

The velocity-feedforward is designed by moving the mass and tuning the feedforward online. It showed the coulomb friction was most important. Attempts with a viscous friction compensation had no effect on the error. So only coulomb friction is compensated in the velocity-feedforward.
To reduce the error even more, a dither signal is added to the output of the controller. A dither signal is a 'highfrequent' signal that lets the actuator vibrate to overcome the stick slip. After online tuning of the frequency and amplitude of the signal a dither sine with amplitude 0.2 and a frequency of 60 rad/sec gave the best results.

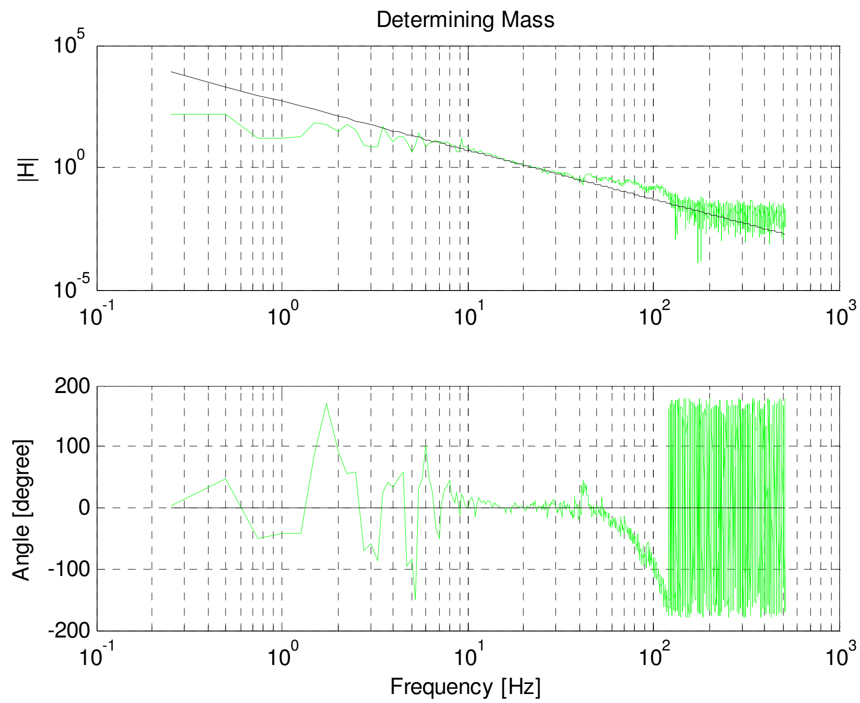

Figure 4.6: bode plot printer 2

Due to a lack of time no position-feedforward is designed. This could improve the accuracy a lot. The preferred position of the motor can be seen very well in the error, as can be seen in figure 4.7. The error has been measured with a trajectory with a velocity of 8 mm/min and with feedforward and dither signal in the controller. Although there are some small things that can be improved to reduce the error, the limit of the resolution of the encoders is also coming in sight, as can be seen in figure 4.8. Steps can be easily distinguished in the error. This points to individual encoder counts. An encoder count equals 42.7e-3 mm.
The maximum error at the printer is about 0.5 mm. Because the position is measured at the printer, and not at the needle, the exact error cannot be given. The ratio between the printer and the needle is 3, so the error will be approximately 0.2 mm.

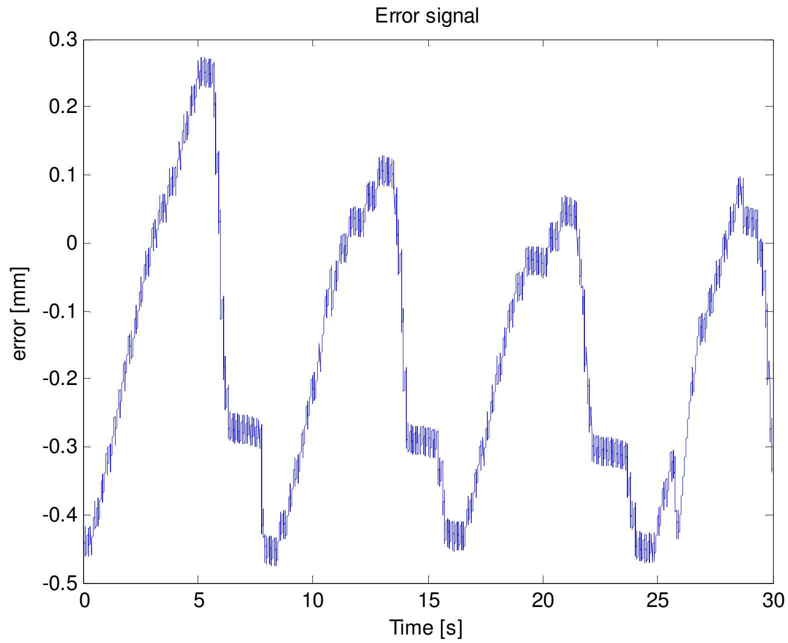

Figure 4.7: error signal

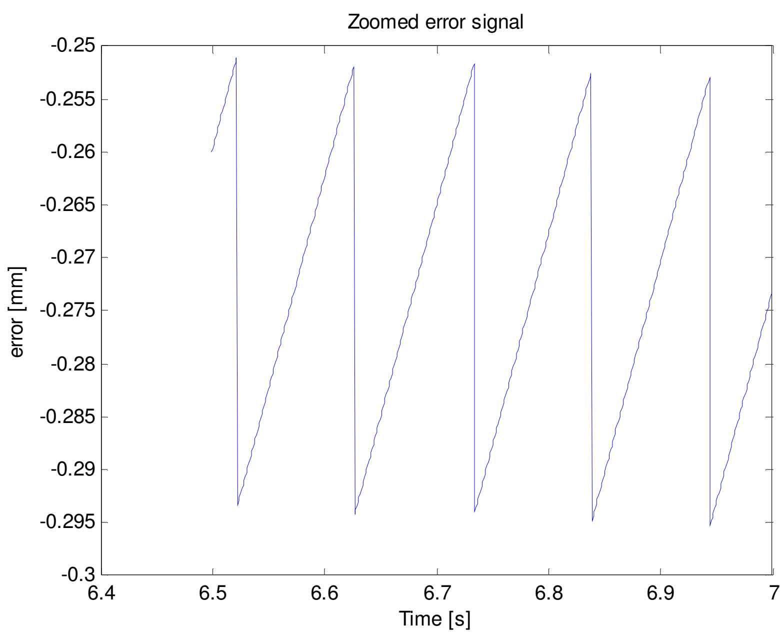

Figure 4.8: zoomed error signal

4.2 Control of the z-direction

A FRF measurement is a good way to identify a system. The problem with the z actuation is that no position sensor is available. Later on in the project there was a sensor: the reflected power of the plasma needle. However, the signals from the powerheads are so noisy they are not suitable for system identification. So the controller for the z actuation had to be designed in another way.
The first measurement that has been done was to determine the friction. This has been done by increasing the voltage slowly, until the actuator started moving. The z actuation seems to have a lot of friction, just like the x and y actuators. The voltage at which the actuator starts moving is not the same for positive and negative direction. We assumed the friction is the same for both directions. The offset that occurred during the measurements is assumed to be caused by gravitational forces. The coulomb friction feedforward and the gravitational compensation are identified now.
Together with the gravitational compensation, the mass is also known. Gravitational forces equal m*g. Although the estimation of the mass will not be very accurate, it is a good magnitude estimation. Another assumption that has been made is that it is a pure mass system. So the transfer function equals $1/(m*s^2)$. With this information a low-bandwidth controller can be made, because the resonance frequencies are assumed to be higher than 10 Hz. This should be enough, because the plasma needle only moves with 8 mm/min.

The position sensor signal in z direction consists of the quotient of the forward and reflected power of the plasma needle. As can be seen in figure 4.9 this sensor is not very accurate, but should be accurate enough for its purpose.
A big problem of this sensor is that the signals from the powerheads are very noisy. To be able to use the signals, a 2^{nd} order low-pass filter is used. The effect of this filter on the noise is shown in figure 4.10 for several cut-off frequencies. A filter with a cut-off frequency at 4 Hz smoothes the signal well. It averages well and does not have a lot of lag. All filters have a damping of 0.4.

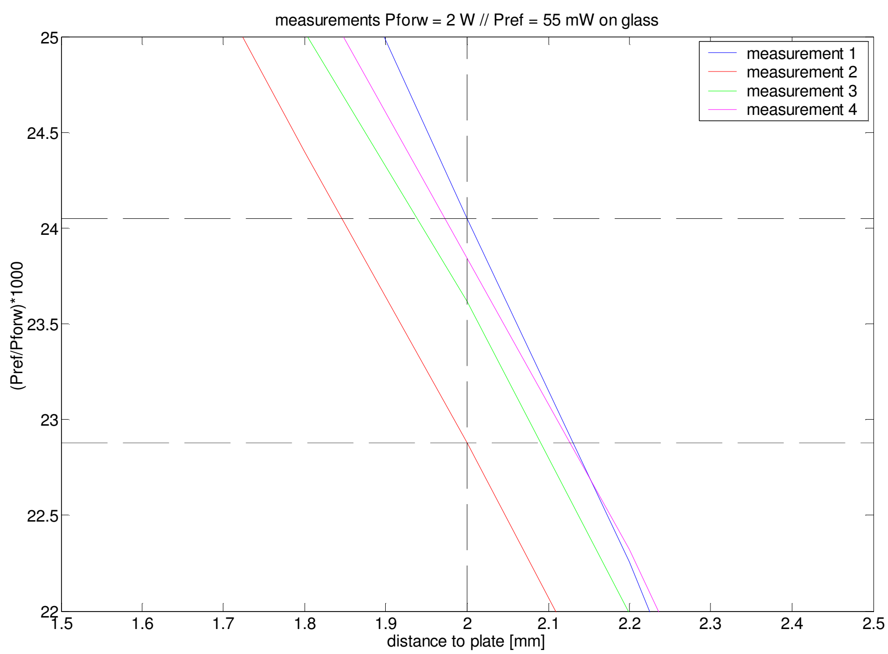

Figure 4.9: deviation of quotient after 5 hours op warming up

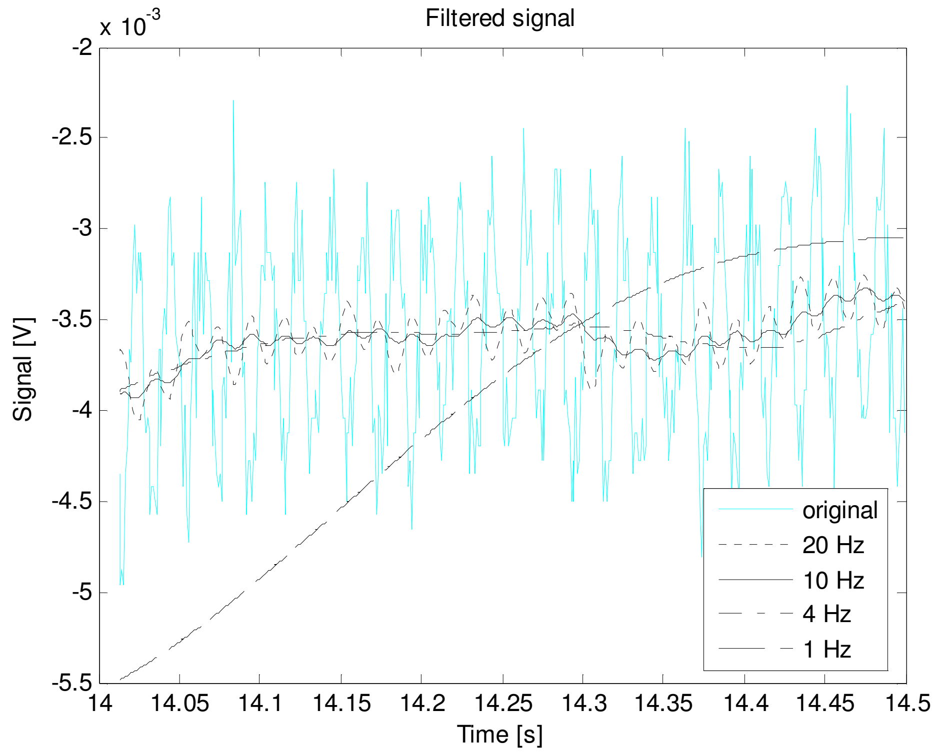

Figure 4.10:Filtered signal with different filters

The bandwidth of the controller is chosen at 1 Hz. The controller is a lead controller. Together with the low-pass filter with a cut-off frequency at 4 Hz this still gives a nice phase margin at 1 Hz (figure 4.11). Figure 4.12 shows a Nyquist plot of the controller together with the low-pass filter and the theoretical system. Because of the amount of assumptions the system should be robust. As can be seen in the figure, that is the case here.

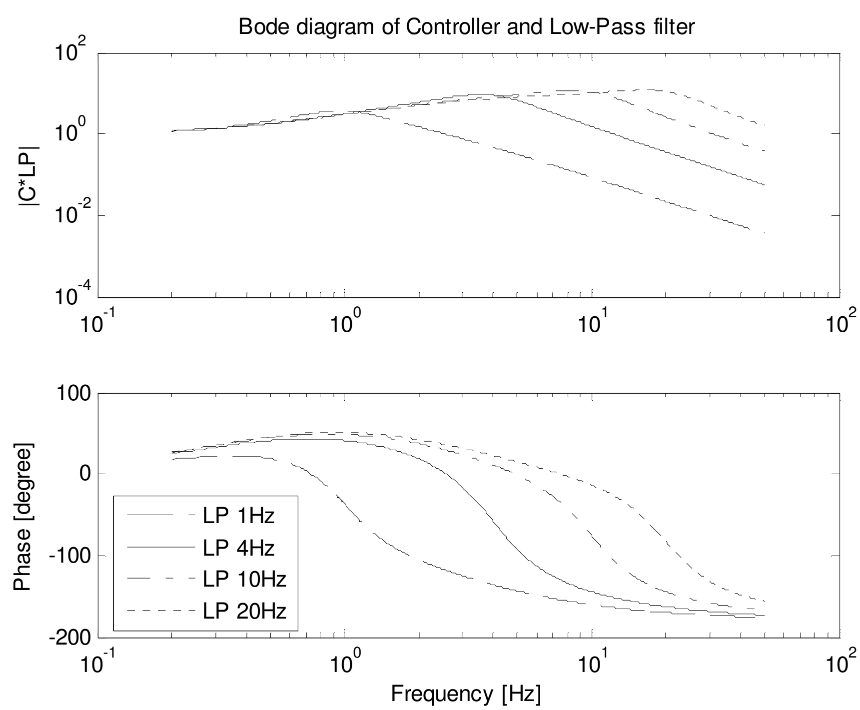

Figure 4.11: bode diagram

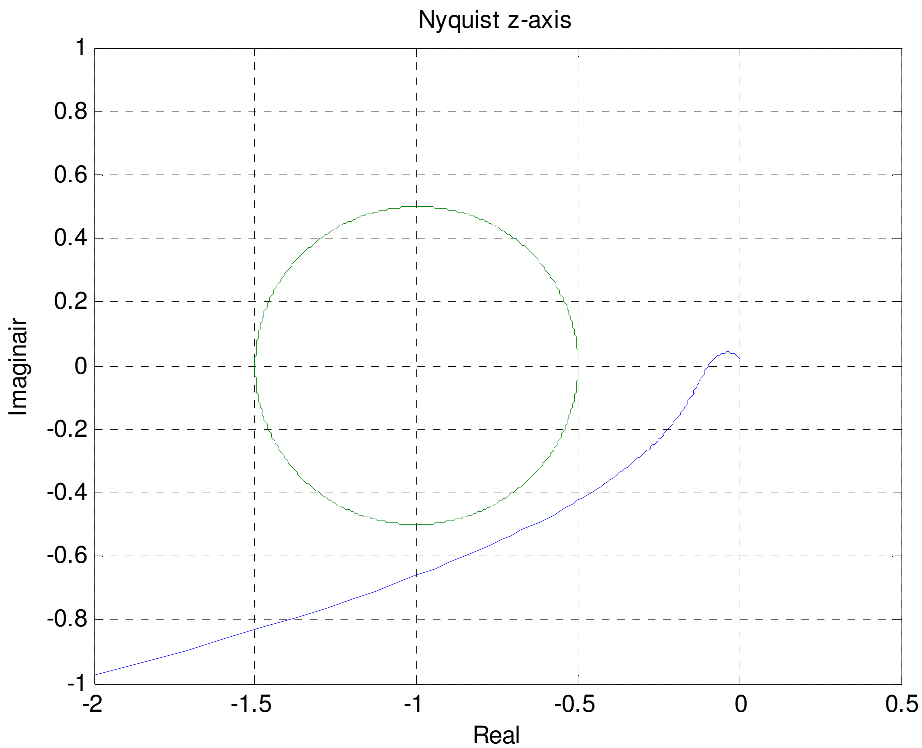

Figure 4.12: Nyquist z-axis

Conclusion and recommendations

During this project research has been done to improve the plasma needle and to design a x, y and z-actuator. The new design for the needle is much smaller and lighter than the old design. Furthermore it uses less helium and power. The new plasma needle can be used as a height sensor within the specifications of 0.1 mm. It is also suitable to be used as a handheld pencil for treatment in the mouth.
Using 2 printers and a CD-Rom drive, a construction to move the new needle has been designed and realized. It has an eigenfrequency of approximately 30 Hz in x- and y-direction. The x- and y-directions are decoupled by using an intermediate body. With this construction it is possible for the plasma needle to be moved in x, y and z-direction. All the requirements for the construction except the accuracy in z-direction are met.

Recommendations

The material of the wire used in the plasma needle may influence the fluctuation of the powers, the exact cause of this effect is not clear, so some research is necessary.
In the measurements it became clear that the forward, as well as the reflected powers varied at one distance in one measurement. This made the quotient inaccurate. The effect only occurred with the new needle, not with the older one. Therefore it is not attributed to the electronics but to the new needle, so research has to be done on plasma generation.
Also a new, more compact matchbox with good possibilities to accurately adjust the forward and reflected power has to be designed. The design should also make the measurements reproducible after a shorter heating up period.
Also a lower reflected power can be obtained. In that case, the optimal amount of forward power can be used to generate plasma.
The radial electrical field around the wire will also have to be investigated, because this affects the thickness of the glass isolation. From this a larger wall thickness for the cover of the needle has to be used. It has to be at least 0.8 mm (see appendix F). In this way, plasma will only be generated at the tip and not earlier downstream.
If possible use air instead of helium to produce plasma with. In the way a helium tube, flexible tube and helium chamber are no longer needed. This makes it possible to reduce the size of the needle. Furthermore, the (quite expensive) helium is no longer needed. A drawback is the higher power needed to sustain plasma in air. In a practical manner, one can think of a female SMC-connector, filled with Teflon. The wire can be covered by glass. When helium is still to be used, make the stainless steel cover of Teflon. This is lighter and can also withstand the sterilisation temperatures (about 150 degrees Celsius)
Now, most measurements are performed on a sheet of glass and some on aluminium with a layer of tape on it. The sensor showed different results of the quotient when different “skins” were used. Testing can also be done on plastic or flesh (like chicken).
Use a movable box onto which electronics can be put. These electronics are the matchbox and source/amplifier (transmitter). It is also possible to put a (small) cannister of helium onto this box. Using an arm, the flexible tube through which the helium flows and the coax cable can be guided. In that way, the doctor can move freely. When the needle is not used, it can be put in a holder.

The actuator is quite large, so a smaller construction has to be designed. Also the stick slip of the printers has to be eliminated. Furthermore the actuator in z-direction has to be identified using a FRF.

Symbols

Symbol	Description	Unit
A	amplitude	[-]
Ø	phase shift	[rad]
ω	angular velocity	[rad/s]
y	sinusoidal function	[-]
Y	phasor representation	[-]
Z	phasor	Ω
R	real part of a phasor	Ω
X	imaginary part of a phasor	Ω
Z_r	impedance resistor	Ω
Z_c	impdance capacitor	Ω
Z_l	impedance inductor	Ω
Z_{tot}	total impedance	Ω
Y	admittance	1/ Ω
Z_k	impedance transmission line	Ω
$\Gamma(x)$	reflection coefficient	[-]
$P_{reflected}$	reflected Power	[W]
$P_{forward}$	forward Power	[W]
m_{eq}	equivalent mass	[Kg]
C_c	equivalent stiffness	[N/m]
f_{eigen}	eigen frequecy	[Hz]
$c_i^{'}$	replacement stiffness	[N/m]
$m_n^{'}$	replacement mass	[kg]

References

[1] I.E. Kieft, N.A. Dvinskikh, J.L.V. Broers, D.W. Slaaf and E. Stoffels. *Effect of plasma needle cultured cells.* Proc. SPIE, 5483:247-251, 2004

[2] R.E.J. Sladek, E. Stoffels, R Walraven, P.J.A. Tielbeek, and R. Koolhoven. *Plasma treatment of caries: a novel method in dentistry.* IEEE Trans. Plasma Sci., 32(4):1540-1543, 2004

[3] Veron, *Cursusboek voor C-zendvergunning,* Arnhem 1980

[4] E. van der Laan, (July 2004) *The development of a smart-scanning probe for the plasma needle.* Verslag: BMT/N 04.01, master thesis, Department of Biomedical Engineering, Eindhoven University of Technology

[5] I. E. Kieft. *Plasma needle: exploring biomedical applications of non-thermal plasmas.* Department Applied Physics, Eindhoven University of Technology

[6] Vink, productkaart kunststoffen 09.04 (WenST)

[7] Concstructie principies 1 bedoelt voor het nauwkeurig bewegen en positioneren, Technisch universiteit Eindhoven, Faculteit Werktuigbouwkunde, sectie Precision engineering

[8] D.C Giancoli. *Physics for scientists and engineers, third edition.* Prentice Hall, Upper Saddle river, New Jersey 07458

[9] *Leidingnetberekening,* RLM 77 ISS, Instituut voor studie en stimulering van onderzoek op het gebied

Appendix A: Used Equipment

Table A.1: used equipment for plasma setup

Equipment	**Manufacturer**	**Comments**
Source	"RF voeding 13.56 MHz/10W/nr. 5" Plasma-naald (RFvoeding)5 Ordernr. 10001568 Bouwjaar 2005	-
Matchbox (large)	"large" matchbox Ewout van der Laan	-
Matchbox (small)	"small" matchbox (black) Plasma-naald (matchbox) Ordernr. 10001568 Bouwjaar 2005	-
Powermeter	"amplifier research" serial number 303217	-
Powerheads (2 pieces)	"amplifier research" model PH2000 serial number 301206 "amplifier research model PH2000 serial number 301209	-
Read-out cables for powerheads (2 pieces)	"amplifier research" model PH2000 serial number 301206 "amplifier research model PH2000 serial number 301209	Cables should only be used with corresponding powerheads
Read-out unit for powers	"amplifier research" model PM2002 Power Meter	-
Mass flow controller	"Brooks Instrument bv" Veenendaal	-
Mass flow controller read-out unit	"Brooks Instrument bv" Veenendaal Brooks 5850 E series	-
Old needles 1 and 2		-
New needles 1 and 2		-

Table A.2: used equipment for x, y and z-actuator

Equipment	Manufacturer	Comments
printers (2 pieces)	HP Deskjet	The first one is of the 800 series, the second of the 900 series
CD-Rom drive	Unknown	-
TUeDACS	TU/e	-
Amplifiers for TUeDACS (3 pieces)	TU/e	-
Laboratory power supply	Voltcraft PS 303 Pro	-

Appendix B: Specifications slides

The slides, which have been used are made by IKO Thompson:
Type: LWL*12 C1R100**BCSH S2

Dimensions slides:

Length slide	42 mm
Length rail	120 mm
Mass slide	35 gram
Mass rail	78 grams
Material rail	high carbon steel
Tolerance H	+-0,020 mm
Variation of H	0,020 mm
Parallelism slide	4e-6 m

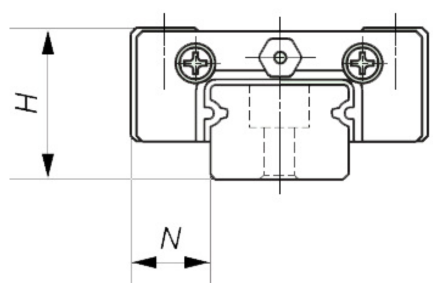

Figure B.1: cross-section slide

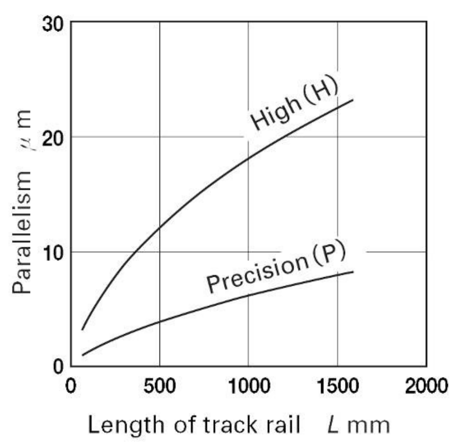

Figure B.2: parallelism slide

Appendix C: measurements belt

The measured belt is of a HP DeskJet printer, type 840C

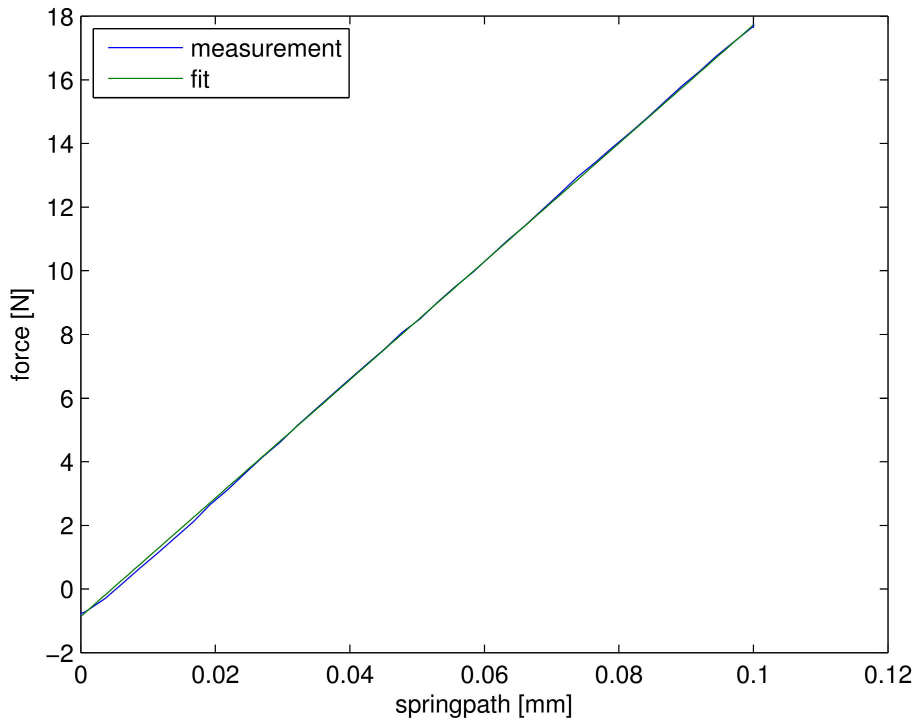

Figure C.1: force against springpath

Appendix D: overview masses and stifnesses

Table D.1: description of masses printer 1

Symbol	description	Mass [kg]	Symbol reduced mass	Reduced mass [kg]
M_1	Slide	469e-3	M'_1	469e-3
M_2	Assistant slide	115e-3	M'_2	115e-3
M_3	Bar	9e-3	M'_3	9e-3
M_4	Lever part 1	41e-3	M'_4	41e-3
M_5	Lever part 2	21e-3	M'_5	186e-3
M_6	Bar	18e-3	M'_6	162e-3
M_7	Printer head	148e-3	M'_7	1332e-3
M_8	Belt	1e-3	M'_8	9e-3

Table D.2: description of stiffnesses printer 1

Symbol	description	Stiffness [N/m]	Symbol reduced stiffness	Reduce stiffness [N/m]
C_{12}	Spring	1.0e5	C'_{12}	1.0e5
C_{23}	Ball head	1.0e5	C'_{23}	1.0e5
C_3	Bar	3.68e6	C'_3	3.68e6
C_{34}	Ball head	1.0e5	C'_{34}	1.0e5
C_4	Lever part 1	0.48e6	C'_4	0.48e6
C_5	Lever part 2	1.78e4	C'_5	1.60e5
C_{56}	Ball head	1.0e5	C'_{56}	9.0e5
C_6	Bar	1.055e6	C'_6	9.50e6
C_{67}	Ball head	1.0e5	C'_{67}	9.0e5
C_8	Belt.	1.86e5	C'_8	1.67e6

Table D.3: description of masses printer 2

Symbol	description	Mass [kg]	Symbol reduced mass	Reduced mass [kg]
M_1	Slide	559e-3	M'_1	559e-3
M_2	Bar	10e-3	M'_2	10e-3
M_3	Lever part 1	41e-3	M'_3	41e-3
M_4	Lever part 2	21e-3	M'_4	186e-3
M_5	Bar	17e-3	M'_5	162e-3
M_6	Printer head	148e-3	M'_6	1332e-3
M_7	Belt	1e-3	M'_7	9e-3

Table D.4: description of stiffnesses printer 2

Symbol	description	Stiffness [N/m]	Symbol reduced stiffness	Reduce stiffness [N/m]
C_{12}	Ball head	1.0e5	C'_{12}	1.0e5
C_2	Bar	3.68e6	C'_2	3.68e6
C_{23}	Ball head	1.0e5	C'_{23}	1.0e5
C_3	Lever part 1	0.48e6	C'_3	0.48e6
C_4	Lever part 2	1.78e4	C'_4	1.60e5
C_{45}	Ball head	1.0e5	C'_{45}	9.0e5
C_5	Bar	1.23e6	C'_5	1.11e7
C_{56}	Ball head	1.0e5	C'_{56}	9.0e5
C_7	Belt	1.86e5	C'_7	1.67e6

Appendix E: Dynamic model

To get insight in the dynamic properties of the x,y,z-actuator, a dynamic model has been made. In this model the masses, stiffnesses and clearances are determined or estimated. In this way the lowest natural frequency can be determined. In figure E.1 an overview of the model of printer 1 is given. This printer actuates the plasma needle in y direction. Printer 2 actuates the printer in x direction. An overview of this dynamic model can be found in figure E.2. The explanation of the different masses and stifnesses is given in tables in appendix D.

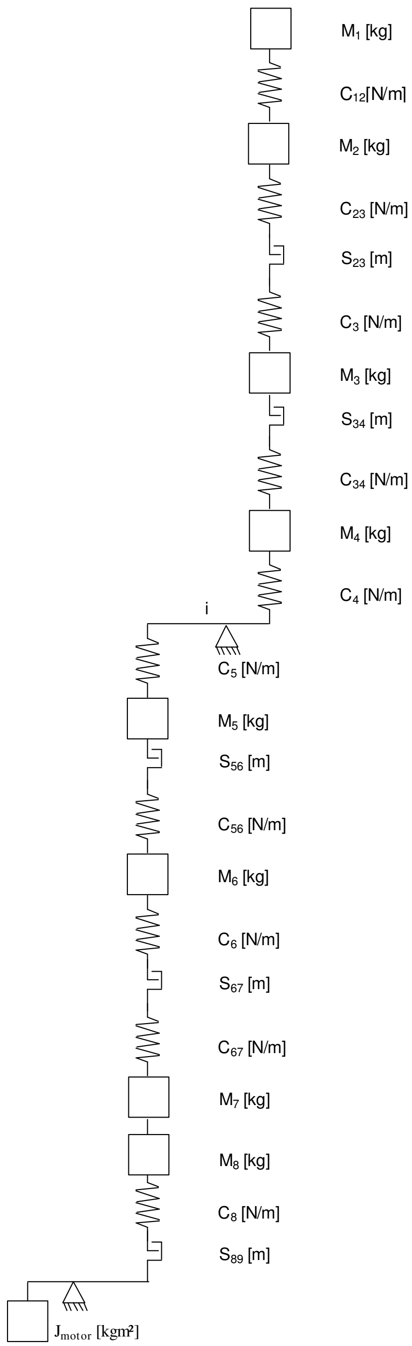

Figure E.1: dynamic model printer 1

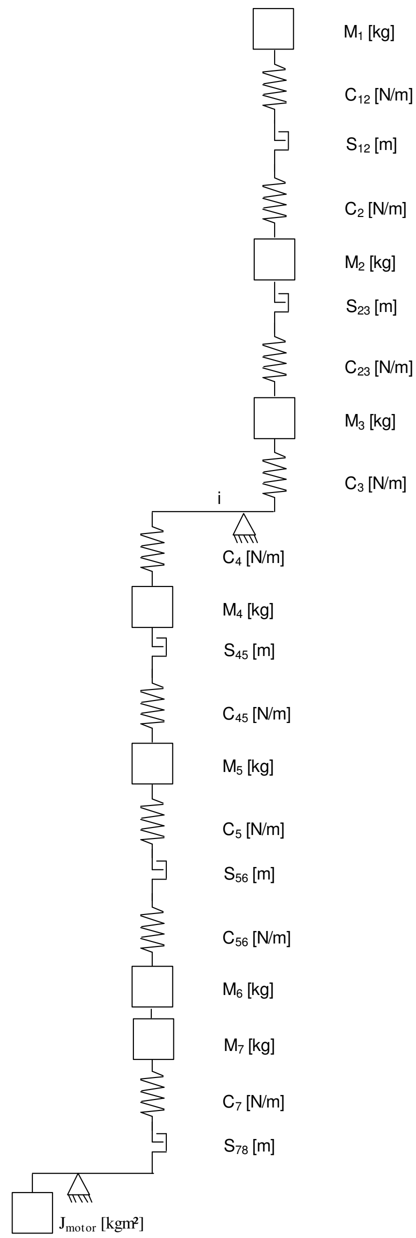

Figure E.2: dynamic model printer 2

Using the method of Rayleigh, the lowest natural eigen frequency was calculated.
To be able to compare different stiffnesses, the ratio of the lever, has to be taken into account. Every mass and stiffness has to be transformed to the value, which you feel at the end of the construction (the place of the plasma-needle). Using formulas [7], the reduction of the mass is equal to;

$$m' = \frac{m}{i^2} \tag{E.1}$$

The reduction of the stiffness is equal to

$$k' = \frac{k}{i^2} \tag{E.2}$$

In formula 1 and 2, the ratio factor i, is equal to

$$i = \frac{out}{in} \tag{E.3}$$

In this situation, the ratio factor for the lever is equal to 0.33.

In Appendix 3 an overview is given of the different (reduced) masses and (reduced) stiffnesses of printer 1 and 2.
The clearances S_{23}, S_{34} S_{56} and S_{67} are the clearances of the ball heads, the clearance S_{89} is the clearance between belt and pulley. These clearances are not taken into account during further calculations.

The stiffness of the ball head is estimated on a value of 1e5 N/m. The stiffness of the belt is measured with a strength tester. Results of this measurement can be found in Appendix 2. The stiffness of belt is equal to 1.86e5 N/m.

For this model it is supposed, the motor is not turning. In this way the motor is the fixed ground. So the area moment of inertia of the motor is not used, just as the ratio of the pulley on the motor.

Appendix F: Calculation of the radial electrical field around the wire

Introduction
In order to make sure plasma is generated only at the tip of the needle and not inside the needle, a cover is needed. The strength of the electrical field is responsible for the generation of plasma. In order to keep this field low (smaller than about 2.1e5 V/m), the dielectric constant of the cover is of importance. In this appendix, a calculation method is provided to calculate the radial electrical field. In this way a lower bound on the wall thickness of the cover can be calculated.

Calculation of the radial electrical field around the covered wire
The voltage and therefore the current produced by the source, alternate with a frequency of 13.56 MHz. This means that the sign of the velocity of the electrons in the tungsten wire alternates very fast. One half of the period, the electrons move in one direction, the other half period they move in the other direction. The current per half wavelength induces a charge of the wire.

To calculate this field, some assumptions have to be done:
1) the thickness of the wire is negligible
2) the phase difference between the voltage and the current is zero
3) the voltage and current follow a sinusoidal behaviour.
4) the relative dielectric constant ε_r of tungsten is in order of magnitude of the dielectric constant of tungsten trioxide ((WO_3) which is about 300 [-].
5) the relative dielectric constant of the glass as has been used is about 6
6) the relative dielectric constants are not a function of frequency

The wavelength of the wave can be calculated with formula F.1 [1]:

$$\lambda_{uncorrected} = \frac{c}{f} \tag{F.1}$$

with:

λ = wavelength of an electro-magnetical wave

c = speed of light in air (equals 3e8 $\frac{m}{s}$)

f = frequency of the by the source produced voltage and current

Because of the dielectric constant of a wire, a reduction factor for the wavelength has to be dealt with. It corrects the wavelength as calculated in formula F.1 with (see formula F.2):

$$\lambda_{corrected} = \lambda_{unccorected} * \frac{1}{\sqrt{\varepsilon_{r\_tungsten}}} \tag{F.2}$$

Furthermore, the charge has to be calculated. The power that is provided by the source is about 10 W. The assumption made is that the power at the tip obeys formula F.3:

$$p(t) = I_m * V_m * \cos(\omega * t + \theta_i) * \cos(\omega * t + \theta_v) \tag{F.3}$$

with:

I_m = amplitude of the current

V_m = amplitude of the voltage

ω = angular frequency

t = time

θ_i = phase shift of the current

θ_v = phase shift of the voltage

To calculate the charge per half wavelength, the duration of a wavelength is required. The half of the period is defined as can be seen in F.4:

$$\frac{T}{2} = \frac{1}{2 * f} \tag{F.4}$$

These starting time and end time of a half wavelength can be used as boundaries of the integration interval. The integration constant has been changed to x, because of the time boundaries used. The charge becomes:

$$Q = \int_{t0}^{t1} p(x)dx \tag{F.5}$$

With the half of the wavelength, the charge of the wire per meter becomes:

$$Labda = \frac{Q}{\lambda}\left[\frac{C}{m}\right] \tag{F.6}$$

The formula of the radial electrical field around a thin, infinitely long wire is:

$$E(r) = \frac{Labda}{2 * pi * \varepsilon_{r\_dielectricum} * r} \tag{F.7}$$

With the use of these formulas, one can finally calculate the radial electrical field.

$$\frac{T}{2} = \frac{1}{2 * f} \approx 3.69e-8$$

$$Q = \int_{t0}^{t1} p(x)dx = 0.0222$$

$$Labda = \frac{Q}{\lambda} = \frac{0.0222}{3.69e-8} \approx 596.2e3\left[\frac{C}{m}\right]$$

This gives the following result for the radial electrical field and minimal wall thickness when glass and Teflon are used:

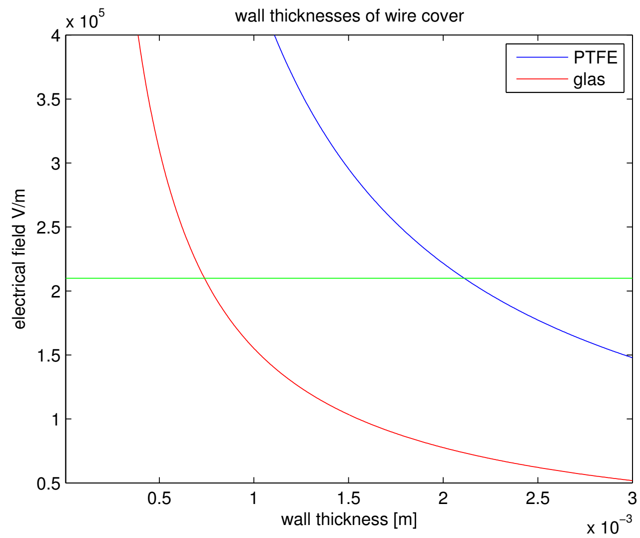

Figure F.1: radial electrical field around the wire using Teflon and glass

In figure F.1 one can see that glass has to be preferred to Teflon. Furthermore, the order of magnitude of the wall thickness of the cover is about 1 mm to reduce the radial electrical field enough. In this way, plasma will be generated only at the tip of the wire. It has to be said that rough assumptions are made, so the values are only lower bounds.

Appendix G: calculations on the helium flow and pressure drop

Calculations
For the helium flow and the pressure drop, calculations have been made. They are listed below.

G.1 Helium flow

The optimal working condition of the needle is dominated by the forward- and reflected power and the velocity of the flow around the tip of the tungsten wire. The helium flow of the old needle is 2 L/min, which with an diameter of 5.5 mm of the Perspex tube, results in a flow velocity of:

$$u_{helium} = \frac{\dot{V}}{A} = \frac{\dot{V}}{\frac{\pi}{4}D^2} = \frac{\frac{2e-3}{60}\left[\frac{m^3}{s}\right]}{\frac{\pi}{4}(5.5e-3)^2\left[m^2\right]} = 1.4\left[\frac{m}{s}\right] \qquad \text{(G.1)}$$

Using the same formula and flow velocity but a diameter of the tube of only 3 mm, the flow becomes about 0.6 L/min. This is a reduction of the helium consumption with about 300 %.

G.2 Pressure drop

Although the needle is operated at almost atmospherical pressure, the pressure drop over the flexible tube and the holes in the Teflon cap is calculated.

The flow is laminar when the Reynolds number considering the diameter is smaller than 2300, see formula G.2 [9]:

$$\mathrm{Re}_D = \frac{u_{helium} * D}{\nu} \qquad [-] \qquad \text{(G.2)}$$

with:

u_{helium} = velocity of the helium flow $\left[\frac{m}{s}\right]$

D = diameter of the (flexible) tube $[m]$

ν = kinematical viscosity $\left[\frac{m^2}{s}\right]$

When it is assumed that the velocity of the gas is never larger than 10.61 m/s (as is in the flexible tube) at a diameter of 2 mm, the Reynolds number will be:

$$\mathrm{Re}_D = \frac{10.61 * 2e-3}{20e-6} = 1061 < 2300$$

This means the flow is laminar. For the pressure drop, formula G.3 is valid:

$$\Delta P = \lambda * \frac{L}{D} * \frac{\rho * u_{helium}^{\;2}}{2} \tag{G.3}$$

with:

ΔP = pressure drop over (flexible) tube $[Pa]$

λ = $\frac{64}{\mathrm{Re}_D}$ friction factor $[-]$

L = length of the (flexible) tube $[m]$

ρ = density of the medium $\left[\frac{kg}{m^3}\right]$

For the flexible tube (of about 1 meter length and with an inner diameter of 2 mm), this means a pressure drop of:

$$u_{helium} = \frac{\dot{V}}{A} = \frac{\dot{V}}{\frac{\pi}{4}D^2} = \frac{\frac{2e-3}{60}}{\frac{\pi}{4}(2e-3)^2} = 10.61\left[\frac{m}{s}\right]$$

$$\mathrm{Re}_D = \frac{u_{helium} * D}{\nu} = \frac{10.61 * 2e-3}{20e-6} = 1061[-]$$

$$\Delta P = \lambda * \frac{L}{D} * \frac{\rho * u_{helium}^{\;2}}{2} = \frac{64}{1061} * \frac{1}{2e-3} * \frac{0.178 * (10.61)^2}{2} \approx 302[Pa]$$

By using the same formulas, the pressure drop over the 4 holes (of about 10 mm length and a diameter of 1 mm) in the Teflon cap can be calculated:

$$\Delta P = \lambda * \frac{L}{D} * \frac{\rho * u_{helium}^{\;2}}{2} = \frac{64}{416} * \frac{1e-2}{1e-3} * \frac{0.178 * (8.3)^2}{2} \approx 9.4[Pa] \text{ per hole.}$$

The pressure drop over the blind hole (5.5 mm length and a diameter of 3 mm) in the Teflon cap is:

$$\Delta P = \lambda * \frac{L}{D} * \frac{\rho * u_{helium}^{\;2}}{2} = \frac{64}{707.3} * \frac{5.5e-3}{3e-3} * \frac{0.178 * (4.7)^2}{2} \approx 0.33[Pa]$$

When summed, the total pressure drop is about 340 Pa. This is indeed negligible when compared to the ambient pressure. This means that the scattering of the helium in the chamber of the needle will be done easily. Furthermore, a pump is not needed and almost all helium from the canister can be used.

Appendix H: Measurements plasma needle

See CD-rom file: